Origin of Lower Ordovician dolomites in eastern Laurentia: Controls on porosity and implications from geochemistry

Ebube Azomani [a,*], Karem Azmy [a], Nigel Blamey [a,b], Uwe Brand [b], Ihsan Al-Aasm [c]

[a] Department of Earth Sciences, Memorial University of Newfoundland, 300 Prince Philip Drive, St. John's, NL, Canada A1B 3X5
[b] Department of Earth Sciences, Brock University, St. Catharines, ON, Canada L2S 3A1
[c] Department of Earth and Environmental Sciences, University of Windsor, Windsor, ON, Canada N9B 3P4

a r t i c l e i n f o

Article history:
Received 8 January 2012
Received in revised form
20 October 2012
Accepted 24 October 2012
Available online 13 November 2012

Keywords:
Carbonate diagenesis
Dolomitization
Catoche
Rare earth elements
Fluid inclusion gas analysis
Stable isotopes
Geochemistry
Newfoundland

a b s t r a c t

The Catoche Formation of the St. George Group in eastern Laurentia (western Newfoundland) consists of early Ordovician (Arenigian) shallow marine platform carbonates (w160 m thick), which were extensively dolomitized during the course of their diagenetic history. The dolomites occur as both replacement and pore-filling cements and are a major control on porosity distribution in the formation. The origin and diagenetic history of the Catoche dolomites at Daniel's Harbour (western Newfoundland) were analysed in comparison to equivalent successions at Port au Choix (PaC) and Port au Port Peninsula (PaP) to assay the reservoir potential of these dolomites in eastern Laurentia. Petrographic examination identified at least three generations of dolomites in the Catoche Formation, which are: (1) an early replacement sub- to eu-hedral micritic dolomite (<4 mme30 mm, D1), (2) eu- to sub-hedral dolomite (70 mme1 mm) often with cloudy cores and clear rims (D2), and (3) subhedral to anhedral saddle dolomite cement (200 mme3 mm, D3). The micritic dolomite (D1) exhibits a dull cathodoluminescence (CL) under cathodoluminoscope, whereas dolomite D2 exhibits consistent concentric CL zonation. Some subhedral crystals of D3 appear zoned both in plane polarized light and cathodoluminoscope, otherwise D3 exhibits a dull CL. Stoichiometric dolomite occurs in all three generations with D2 as the dominant dolomite by abundance.

The low strontium (47 ± 25 ppm) content coupled with depleted $\delta^{18}O$ value of dolomitizing fluids (−10 to −11.2& VSMOW) and near-micritic grain size, suggests an early precipitation of dolomite D1 at low temperatures of near-surface conditions from solutions likely formed by mixing of early Ordovician sea and meteoric waters. In contrast, microthermometric measurements of primary two-phase fluid inclusions in dolomite D2 (homogenization temperatures of 102e168 °C with a salinity range of 19.8e25 eq wt% NaCl) and dolomite D3 (homogenization temperatures of 158e190 °C with a salinity range of 20.2e22.2 eq wt% NaCl), suggest that both dolomite generations were generated in mid to deep burial settings from high salinity, low temperature (<200 °C) hydrothermal fluids likely under suboxic conditions. This is consistent with the low Sr concentrations for D2 (36.4 ± 8 ppm) and D3 (38.7 ± 9 ppm), $\delta^{18}O$ values of dolomitizing fluids for D2 (þ2.1 to þ8.1&, VSMOW) and D3 (þ6 to þ8.1& VSMOW), coupled with Fe contents of D2 (1684 ± 1096 ppm) and D3 (1783.7 ± 618 ppm) as well as the respective Mn (D2 ¼ 131.2 ± 50 and D3 ¼ 197.5 ± 55 ppm) concentrations.

SREE and shale normalized (REE_{SN}) values of Catoche carbonates indicate enrichment in rare earth element (REE) composition of the earliest calcite (C1) relative to those of Arenig seawater, whereas the REE_{SN} profiles of the dolomite generations mimic that of calcite C1. The Ce $(Ce/Ce^*)_{SN}$ and La $(La/La^* ¼ Pr/Pr^*)_{SN}$ anomalies of the Catoche dolomites are consistent with precipitation in equilibrium with source fluids in slightly oxic to suboxic conditions whereas Eu $(Eu/Eu^*)_{CN}$ anomalies suggest similar source fluids for D2 and D3. Results of fluid inclusion gas analysis are consistent with petrographic features and geochemical compositions and support the exclusion of magmatic fluids during dolomitization. Visual estimates of porosity (f) from thin sections indicate four porous (f ¼ 4e12) horizons. Vugs and intercrystalline pores are two types of porosity associated with the dolomites with the latter being the dominant type and associated mainly with dolomite D2.

* Corresponding author. Tel.: þ1 709 730 1875.
E-mail address: ebube.azomani@mun.ca (E. Azomani).

0264-8172/$e see front matter © 2012 Elsevier Ltd. All rights reserved.
http://dx.doi.org/10.1016/j.marpetgeo.2012.10.007

1. Introduction

Dolomitization of carbonates in sedimentary sequences have been the focus of many studies particularly in the last few decades. Chemical reactions between magnesium-bearing solutions and calcium carbonate sediments form dolomites via dolomitization. Several models have been put forth to explain the mechanism(s) via which dolomitization occurs, however all models must explain the source of magnesium and method(s) of pumping dolomitizing fluids through pore spaces of rocks. Dolomitization is a significant diagenetic process that influences porosity development and hence the flow of hydrocarbon in carbonate reservoirs. The occurrence of major hydrocarbon accumulations in Palaeozoic hydrothermal dolomites on the eastern Laurentian margin have recently directed studies to western Newfoundland (cf. Haywick, 1984; Lane, 1990; Cooper et al., 2001; Lavoie et al., 2005; Azmy et al., 2008, 2009; Conliffe et al., 2009; Azmy and Conliffe, 2010). Hydrothermal dolomites are formed under burial conditions from high salinity fluids at temperatures higher than the ambient temperature of the host formation (e.g., Davies and Smith, 2006). Temperature(s) of dolomitization must be at least 5 ^{o}C greater than the maximum burial temperature of the host formation for the resultant dolomites to be classified as hydrothermal in origin (e.g., Davies and Smith, 2006; Conliffe et al., 2010).

The Catoche Formation of the St. George Group in western Newfoundland consists of subtidal carbonate sediments that were affected by dolomitization during the course of its burial. The process of dolomitization in the Catoche Formation was pervasive and independent of lithology or stratigraphic position in the sequence as well as geologic structures (Knight et al., 2007, 2008; Azmy et al., 2008, 2009; Conliffe et al., 2009, 2010; Azmy and Conliffe, 2010). Hydrothermal fluids played an important role in this process and the resulting dolomites exhibit a major control on the distribution of porosity in the St. George Group carbonates (Azmy et al., 2008, 2009; Conliffe et al., 2009, 2010; Azmy and Conliffe, 2010). The porosity associated with the dolomites of the St. George Group coupled with the geological proximity of the Cow Head Group (organic-rich shales), presence of structural and stratigraphic traps, as well as reported seeps containing live oil, suggests that the St. George Group and porous equivalent Lower to Middle Ordovician carbonates at Daniels Harbour and neighbouring areas are potential reservoirs for hydrocarbons (Fowler et al., 1995; Stockmal et al., 1998; Cooper et al., 2001; Azmy and Conliffe, 2010; Knight et al., 2007, 2008).

The current study focuses on the Catoche Formation (upper St. George Group) at Daniel's Harbour on the Northern Peninsula in western Newfoundland and the main objectives are:

- To decipher and describe the origin and diagenetic history of the dolomites in the formation.
- To evaluate the reservoir characteristics of Catoche carbonates and the hydrocarbon potential of the succession.
- To correlate results from current study with other successions of the Catoche Formation across western Newfoundland to better understand the pattern of porosity distribution.

2. Geological setting

The St. George Group of western Newfoundland extends approximately 400 km from the Port au Port Peninsula in the south to Cape Norman on the Great Northern Peninsula (Fig. 1). It consists

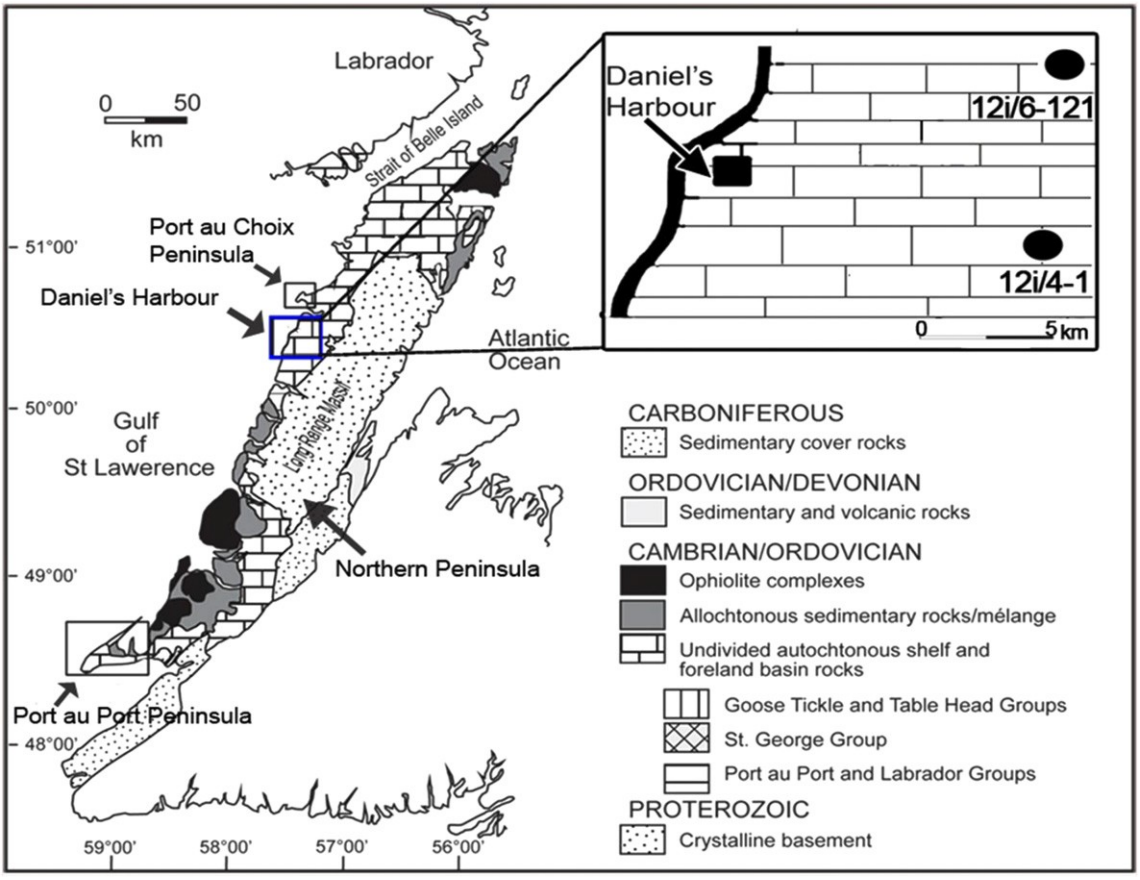

Figure 1. Map of Western Newfoundland showing approximate locations of investigated cores 12i/4-1 and 12i/6-121 near Daniels Harbour and the locations of the counterpart sections in Port au Choix and Port au Port Peninsula (modified Zhang and Barnes, 2004). See text for details.

mainly of an alternating succession of dolomitized early Ordovician (Tremadocian to Arenigian) subtidal and peritidal carbonates. These warm, shallow-water early Ordovician carbonates are divided into two third-order sequences (Knight and James, 1987).

The Laurentian palaeoplate developed by active rifting during the late Precambrian around 570e550 Ma (Cawood et al., 2001) and formed a passive pre-platform shelf that was covered by clastics (James et al., 1989; Cawood et al., 2001). A major transgression along the eastern platform margin of Laurentia during the early Ordovician resulted in the accumulation of thick carbonate deposits which formed a carbonate platform (Wilson et al., 1992; Smith, 2006; Knight et al., 2007, 2008). High-energy Cambrian carbonates of the Port au Port Group were buried by low-energy early Ordovician carbonates of the St. George Group in western Newfoundland (Knight et al., 2007, 2008). Subsequently, tectonic activity led to uplift, exposure and erosion of the carbonate platform resulting in the St. George and Boat Harbour unconformities, with the former marking the upper boundary of the St. George Group and a shift from a passive margin to an active foreland basin (James et al., 1989; Knight et al., 1991, 2007; Cooper et al., 2001). Both unconformities also mark the end of two megacycles (Knight and James, 1987). The St. George Group from bottom to top consists of the Watts Bight, Boat Harbour, Catoche and Aguathuna Formations (Fig. 2) and represents an alternating succession of subtidaleperitidalesubtidaleperitidal carbonate sediments respectively (Knight et al., 2008; Lane, 1990; Haywick, 1984). The Watts Bight and Boat Harbour Formations represent the lower Tremadocian megacycle whereas the Catoche and Aguathuna Formations represent the upper Arenigian megacycle (Knight and James, 1987; Conliffe et al., 2010; Azmy and Conliffe, 2010).

The Catoche Formation rests conformably on the Barbace Cove Member of the Boat Harbour Formation and is overlain by the Aguathuna Formation. It is w160 m thick at Port au Choix (its type area) and consists of a lower well-bedded, fossiliferous, bioturbated grey limestone about 120 m and an upper dolostone about 40 m. However, on the Port au Port peninsula, the formation in ascending order, consists of a lower limestone (w70 m), a middle dolostone (w50 m), and the Costa Bay Member (w40 m). The Costa Bay Member of the Catoche Formation is a distinctively white limestone, which occurs on the Port au Port Peninsula (and adjacent areas) and on the three thrust stacks that deform the shelf rocks (Knight et al., 2007). It has been mapped across western Newfoundland and correlated with the upper (w40 m) dolostone of the succession at Port au Choix (Knight, 1986, 1987, 1994, 1997; Baker and Knight, 1993; Knight et al., 2007). The upper 40 m of the Catoche Formation at Port au Choix is a series of cyclic, shallowing upward, metre-scale peloidal grain stones interpreted as peloidal sand shoals that have been extensively dolomitized (Knight, 1991; Knight et al., 1991, 2007; Baker and Knight, 1993). Estimates of the maximum burial temperature of the Catoche Formation using conodont alteration indices (CAI), acritarch alteration indices (AAI) and random graptolite reflectance data (GRo), indicates higher maximum burial temperatures on the Northern Peninsula relative to the Port au Port Peninsula (Nowlan and Barnes, 1987; Williams et al., 1998). Maximum burial temperatures are <75 °C, 115e120 °C and 120e125 °C at Port au Port Peninsula, Daniel's Harbour and Port au choix respectively (Nowlan and Barnes, 1987; Williams et al., 1998; Conliffe et al., 2010). The Catoche Formation is believed to be Arenigian (Knight et al., 2007; Ji, 1989; Ji and Barnes, 1989; Boyce, 1989; Lane, 1990; Greene, 2008).

3. Methodology

The Catoche Formation was examined in core 12i/4-1 (50.93 m, spanning the Upper Catoche) and core 12i/6-121 (103.7 m, spanning the Lower Catoche) both drilled near Daniel's Harbour on the Northern Peninsula (Fig. 1; 50°14′31″ N, 57°30′52″ W; NAD 83 and 50°17′38″ N, 57°27′50″ W; NAD 83). Core 12i/4-1 was drilled by US Borax and Chemical Corporation in 1981 whereas core 12i/6-121 was advanced by NFLD Zinc mines in 1989 (http://gis/geosurv.gov.nl.ca). The composite core represents a complete section of the Catoche Formation (w154.63 m). Ninety-two samples were taken for analysis at 2 m or less intervals (Appendix 1; Fig. 2).

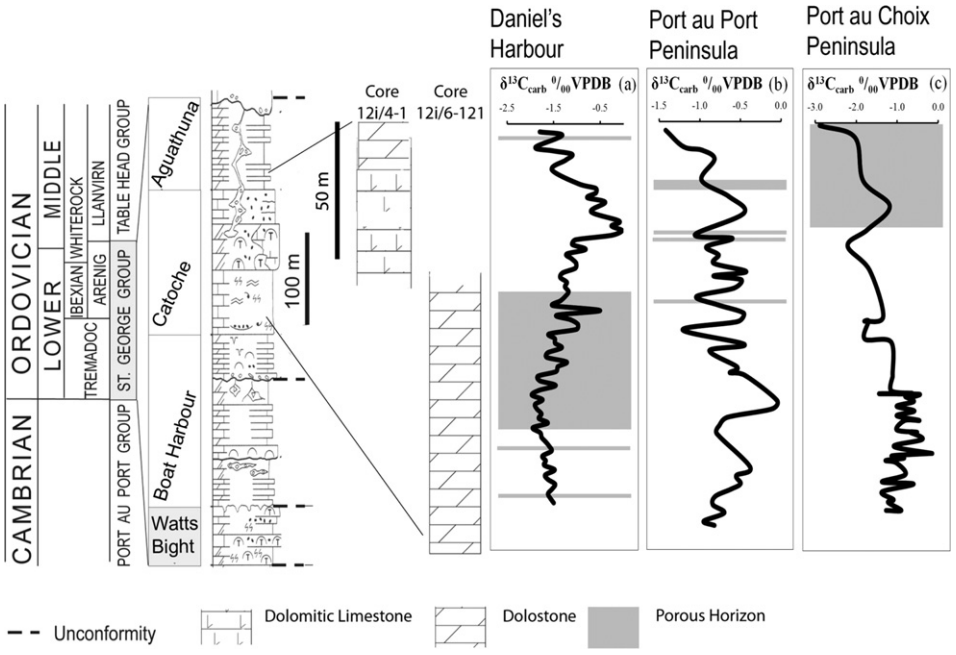

Figure 2. Simplified stratigraphic diagram of the St George Group (Modified from Azmy and Conliffe, 2010) showing the $\delta^{13}C$ profiles and porosity variations within the Catoche carbonates at (A) Daniel's Harbour (current study), (B) Port au Port Peninsula (Conliffe et al., 2012), (C) Port au Choix (Greene, 2008).

Thin sections were stained with Alizarin Red-S and potassium ferricyanide solutions (Lindholm and Finkelman, 1972) and examined under standard polarizing microscope and cathodoluminoscope for petrographic features. A mirror-image slab of each thin section was also polished and cleaned with de-ionized water to be utilized for microsampling and geochemical analyses of the different carbonate generations. Cathodoluminescence was performed using a Technosyn cold cathodoluminoscope operated at ~12 kV accelerating voltage and ~0.7 mA gun current intensity, whereas ultraviolet luminescence was performed using a CRAIC-QDI 202 UV unit mounted on a Zeiss imager D1m microscope.

Microthermometric fluid-inclusion analyses were performed on double polished wafers (approximately100 μm thick) using a Linkam THMSG600 heating-freezing stage. Calibration with precision of ±0.2 °C at −56.6 °C and ±1 °C at 300 °C was conducted using synthetic H_2O and CO_2 fluid inclusion standards. The initial melting temperatures (T_i), last ice melting (T_m (ice)) and the homogenization temperatures (T_h) were measured in primary two-phase fluid inclusions following procedures outlined by Shepherd et al. (1985). Aqueous fluid salinities were calculated using T_m (ice) and the equation of Bodnar (2003).

Polished slabs were washed with deionized water and dried overnight at 50 °C prior to microsampling. Approximately 4 mg were microsampled from the cleaned slabs with a low-speed microdrill. For Carbon and Oxygen isotope analyses, about 200 μg of samples were reacted in an inert atmosphere with ultra-pure concentrated orthophosphoric acid at 50 °C in a Thermo-Finnigan Gas bench II. The CO_2 produced from the reaction was automatically flushed through a chromatographic column and delivered to the source of a ThermoFinnigan DELTA V plus isotope ratio mass spectrometer in a stream of helium, where the gas was ionized and measured for isotope ratios. Analytical errors of better than 0.1‰ (2σ) for the analyses were determined by repeated measurements of NBS-19 ($\delta^{18}O$ = −2.20‰ and $\delta^{13}C$ = +1.95‰ vs. VPDB) and L-SVECS ($\delta^{18}O$ = −26.64‰ and $\delta^{13}C$ = −46.48‰ vs. VPDB) as well as internal standards during each run. For elemental analyses, about 4 mg of a subset of samples was digested in 2.5% (v/v) pure HNO_3 acid (Coleman et al., 1989) and analysed for Ca, Mg, Sr, Mn and Fe as well as rare earth elements (REE) using a HP 4500 plus ICP-MS at Memorial University of Newfoundland. The relative uncertainties of these measurements are better than 4% using DLS 88a-4 and CCH-1-4 as standards. Calculations of major and trace element concentrations are based on an insoluble residue-free basis (100% soluble dolomite or calcite). REE concentrations are normalized based on Post-Archean Australian Shale (McLennan, 1989) and chondrite values (Bau and Dulski, 1996), whereas anomalies of Cerium $(Ce/Ce^*)_{SN} = Ce_{SN}/(0.5La_{SN} + 0.5Pr_{SN})$, Lanthanum $(Pr/Pr^*)_{SN} = Pr_{SN}/(0.5Ce_{SN} + 0.5Nd_{SN})$, and Europium $(Eu/Eu^*)_{CN} = Eu_{CN}/(0.67Sm_{CN} + 0.33Tb_{CN})$ were calculated with the formulae of Bau and Dulski (1996).

The procedure applied for fluid-inclusion gas analysis was described by Norman et al. (1996, 1997, 2002), Norman and Blamey (2001), Norman and Moore (2003) and Parry and Blamey (2010). Approximately 2 g of Samples were mildly crushed by hand and sieved in a 30-mesh sieve with the −30-mesh fraction discarded. The +30 mesh size fraction was first washed in 20% KOH, agitated then decanted. The grains were washed several times in excess amount of 18 MΩ deionized water and air-dried. Gas analyses were conducted with a dual quadrupole mass spectrometer system (two Prisma spectrometers) using the crush-fast scan method (Norman et al., 1996, 1997, 2002; Norman and Blamey, 2001; Norman and Moore, 2003; Parry and Blamey, 2010). The method requires 150 mg of prepared samples and uses 6 to 10 incremental crushes in a vacuum ~10^{-8} Torr to open multiple fluid inclusions thereby releasing gases which are analysed with the mass spectrometers. Species measured includes H_2, He, CH_4, H_2O, N_2, O_2, H_2S, Ar, CO_2, SO_2, C_2–C_4 alkanes and alkenes, and C_6H_6. The system is calibrated with commercial gas mixtures, in-house standards, and natural fluid inclusion standards. Precision and accuracy vary with species. H_2 could be reliably detected at 50 ppm, He at <0.5 ppm. Precision for the major gas species CO_2, CH_4, N_2, and Ar is better than 5%, whereas it is ~10% for the minor species.

4. Results

4.1. Petrography

The Catoche Formation in western Newfoundland consists of limestone and dolostone lithofacies. The limestone lithofacies are fossiliferous and range from mudstone through wacke- and packstone to rare grain stone with lenses and beds of boundstone (Knight et al., 2007; Greene, 2008; Conliffe et al., 2012). The dolostone lithofacies vary from coarse to fine grained (Knight et al., 2007) with some zebra texture in the former.

Petrographic examinations of the Catoche Formation carbonates at Daniel's Harbour indicate that both calcite and dolomite phases are similar to their counterparts at Port au Choix and Port au Port Peninsula (Knight et al., 2007; Greene, 2008; Conliffe et al., 2012). The calcite cement generations, from the oldest to the youngest are: marine micrite and microbial mud (C1), pore-filling equant calcite sparite (C2, 50–200 μm) and coarse blocky calcite (C3, 150–650 μm) often filling vugs and joints (Fig. 3a–c). Calcites C1 and C2 are dull to non-luminescent under the cathodoluminoscope, but calcite C3 exhibits bright orange CL (Fig. 3f). The dolomite generations (Fig. 3d–h), also in the same order, are: dolomicrite (D1), stylolite-associated dolomites (Ds), equant replacive dolomite (D2) and large equant pore-filling replacive saddle dolomite (D3). However, the iron-rich (2'20,000 ppm) pore-filling saddle dolomite reported by Greene (2008) and Knight et al. (2007) at Port au Choix (referred to by them as D5) was not found in the Catoche Formation at Daniel's Harbour. Both calcite and dolomite phases occur as replacement and pore-filling cements and petrographic relationship indicate that calcite C3 postdates all other calcite and dolomite generations (Fig. 3k).

Early dolomite (D1) is ~18.5% by abundance and typically consists of replacive, fabric retentive near-micritic to tightly packed non-planar mosaic crystals with irregular intercrystalline boundaries and range from <4 to 30 μm (Fig. 3d). Dolomite D1 is nonporous (visual estimates) and exhibit dull CL. Stylolite-associated dolomites (Ds) range in size from 60 μm to 175 μm, is associated with stylolites and are cross-contaminated with the residual materials transported along pressure dissolution seams and stylolites. Dolomite Ds samples were excluded in other analyses due to the expected inconsistent signature overprints from insoluble residues and other elements associated with chemical compaction. Similar petrographic features were documented for D1 and Ds dolomites at Port au Choix and Port au Port sections (Knight et al., 2007; Greene, 2008; Conliffe et al., 2012).

Dolomite D2 is the most abundant type of dolomite (making up ~72% of the Catoche carbonates by abundance) and consists of coarse equant euhedral to subhedral crystals ranging from 70 μm to 1 mm. Crystals often have cloudy cores with clear rims under plane polarized light and undulose extinction under crossed polars as well as concentric zoned luminescence under cathodoluminoscope (Fig. 3e, f). It is fabric destructive and likely replaced calcite C1 and/or D1 dolomite. Intercrystalline porosity with estimates up to 12% is associated with D2 dolomite and pores are occasionally filled with bituminous material that fluorescence under UV luminoscope (Fig. 3i, j). Similar features were documented in D2 dolomites at

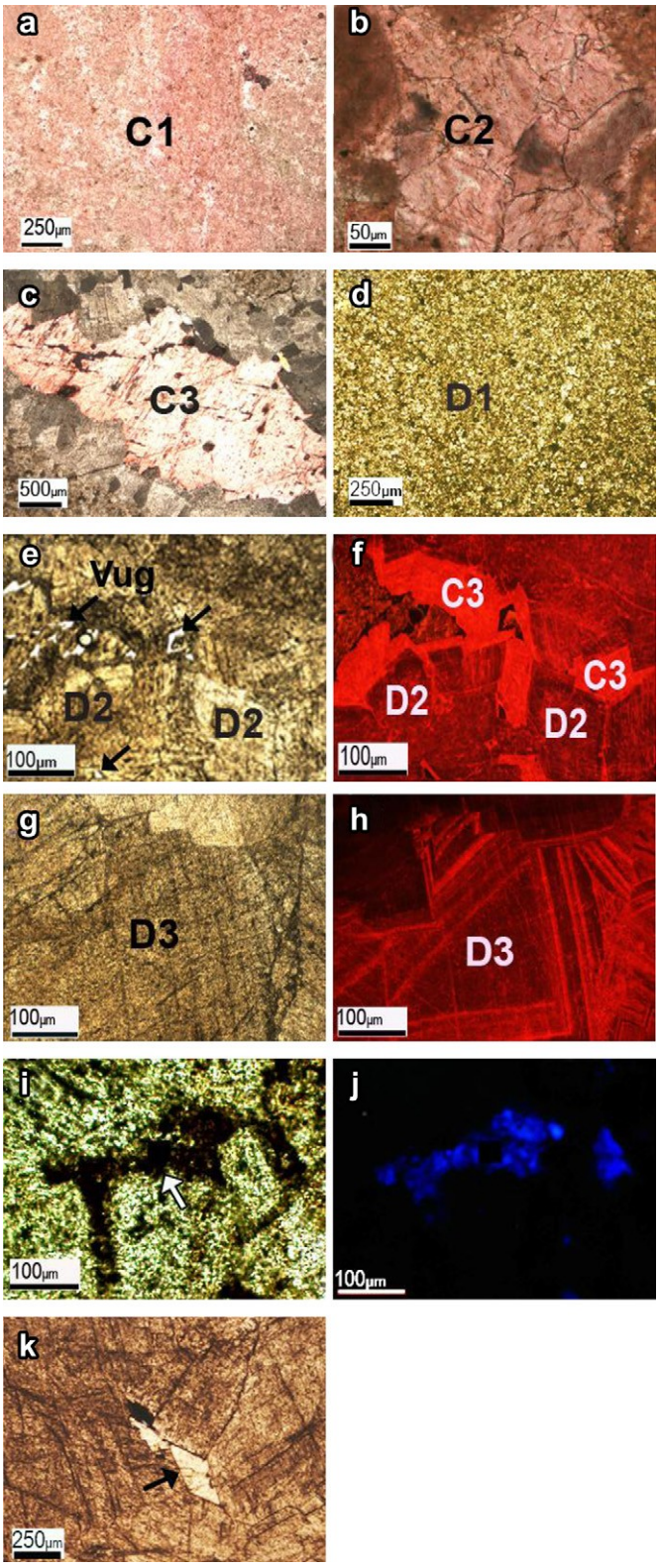

Figure 3. Photomicrographs of petrographic features of Catoche carbonates in the investigated core showing (a) C1 calcite (crossed polars; Sample 4-118), (b) C2 calcite (crossed polars; Sample 4-100), (c) C3 calcite (crossed polarized light; Sample 6-4), (d) D1 dolomite (crossed polars; Sample 6-16), (e) Rhombs of D2 dolomite showing cloudy core with clear rim and intercrystalline pores (arrows) associated with D2 (plane polarized light; Sample 6-4), (f) Cathodoluminescence image of (e) showing concentric zonation CL in D2 and bright orange CL of C3, (g) Subhedral crystal of D3 in crossed polars showing zoning (sample 6-46.5), (h) Cathodoluminoscope image of (g) showing CL-zoning of D3, (i) Sample 6-98 in cross polarized light, and (j) Ultraviolet florescence from sample 6-98, (k) Calcite C3 (arrow) filling intercrystalline pore associated with D3. (For interpretation of the references to colour in this figure legend, the reader is referred to the web version of this article.)

Table 1
Summary Statistics of microthermometric measurements in the Catoche Formation carbonates at Daniels Harbour (current study), Port au Choix and Port au Port equivalent sections (Conliffe et al., 2012).

Host mineral		T_i (°C)	$T_{m\ (ice)}$ (°C)	Eq. wt% NaCl	T_h (°C)
Daniels Harbour (Northern Peninsula)					
D2	n	7	60	60	97
	Mean	−52.3	21.2	23.2	126.6
	S.D.	2.6	2	1.4	12.8
	Max	−48	−16.4	25	168
	Min	−55	−24	19.8	102
D3	n	5	27	27	29
	Mean	−54.3	−18.5	21.3	174.1
	S.D.	3	0.8	0.6	7.6
	Max	−50	−17	22.2	190
	Min	−58	−19.8	20.2	158
C3	n				15
	Mean				101.3
	S.D.				5.2
	Max				108
	Min				92
Port au Choix (Northern Peninsula)					
D2	n	4	17	17	42
	Mean	−54.9	−19.7	22	109
	S.D.	0.5	3.4	2.4	13
	Max	−54.2	−13.6	25.5	134
	Min	−55.3	−24.8	17.4	87
D3	n	6	11	11	16
	Mean	−53.1	10.1	14	118
	S.D.	1	1.8	1.8	10
	Max	−51.7	−7.8	18.4	140
	Min	−54.4	−14.6	11.5	109
C3	n	5	14	14	20
	Mean	−52.8	−21.8	23.6	102
	S.D.	1.7	1.6	1.1	15
	Max	−51.2	−19.7	25	129
	Min	−55.2	−24	22.2	72
Port au Port Peninsula					
D2	n	3	8	8	42
	Mean	−49.8	−12.6	16.5	106
	S.D.	0.7	1.7	1.6	11
	Max	−49	−10.2	19.1	132
	Min	−50.3	−15.6	14.1	90
D3	n	4	10	10	29
	Mean	−51	−17.8	20.7	112
	S.D.	2.3	3.5	2.7	21
	Max	−49.6	−11.2	24.5	147
	Min	−54.5	−23.2	15.7	85
C3	n	5	20	20	29
	Mean	−46.9	−10.2	13.7	116
	S.D.	13.3	3.9	4.2	60
	Max	−23.2	−5	19.1	205
	Min	−53.7	−15.6	7.9	52

Port au Choix and Port au Port peninsula (Knight et al., 2007; Greene, 2008; Conliffe et al., 2012).

The latest dolomite generation (D3) is ~16.3% by abundance and typically consists of pore-filling, coarse, subhedral to anhedral crystals of saddle dolomite, which are up to 3 mm and show undulose extinction (Fig. 3g). Dolomite D3 is generally restricted to vugs and joints and subhedral crystals often appear zoned under crossed polarized light and cathodoluminoscope (Fig. 3g, h). Intercrystalline and vuggy porosity are occasionally associated with D3 particularly with its subhedral crystals. Similar features were also documented in the D3 dolomites in the equivalent sections at

Port au Choix and Port au Port peninsula (Knight et al., 2007; Greene, 2008; Conliffe et al., 2012).

4.2. Fluid inclusions

Primary fluid inclusions were examined in dolomite generations D2, D3 and calcite C3. However, no measurable inclusions were available in D1, and calcites C1 and C2. All microthermometric measurements were performed on primary two-phase (liquid þ vapour) inclusions that occurred mainly in clusters. Care was taken to examine inclusions hosted in the core of crystals or aligned parallel to growth direction as such inclusions are known to retain their primary signatures (Goldstein and Reynolds, 1994). Homogenization temperatures were measured before freezing to avoid stretching of the inclusions by ice formation, an issue described by Lawler and Crawford (1983). Fluid inclusions in dolomites D2 and D3 had consistent liquid: vapour ratios (w0.95) and those found in D3 were larger (>20 mm). The majority of inclusions in the latest calcite cement (C3) were too small to produce reliable results for melting points (and invariably salinity) although some measurements of T_h were obtained. Microthermometric measurements of homogenization temperature ($T_{h,}$ the minimum estimate of entrapment temperature), initial melting temperature (T_i), and final melting temperature of ice (T_m (ice)) with estimated salinity (Bodnar, 2003) were taken from dolomites D2, D3 and calcite C3. The results are summarized in Appendix 2, Table 1 and Figure 4aed. Fluid inclusions in D2 range in size from 2 mm to w20 mm and in D3 from 2 mm to w35 mm. Some inclusion clusters showed evidence of post-entrapment leaking and therefore data were only collected from inclusions that had relatively consistent liquid: vapour ratios and narrow homogenization temperature ranges (usually less than 15 °C).

The mean values of T_h for the respective generations of Catoche dolomites are highest at Daniel's Harbour (Table 1), with values of 126.6 ± 12.8 °C, n ¼ 97 and 174.1 ± 7.6 °C, n ¼ 29 for dolomites D2 and D3 respectively. These temperatures are considerably higher than those of their equivalent dolomites from Port au Choix (D2 ¼ 109 ± 13 °C, n ¼ 42, D3 ¼ 118 ± 10 °C, n ¼ 16) and Port au Port (D2 ¼ 106 ± 11 °C, n ¼ 42, D3 ¼ 112 ± 21 °C, n ¼ 29) sections (Conliffe et al., 2012). The mean salinity of fluid inclusions associated with D2 (Table 1), is similar at Daniel's Harbour (23.2 ± 1.4 eq wt% NaCl, n ¼ 60) and Port au Choix (22 ± 2.4 eq wt% NaCl n ¼ 17) and are higher relative to their counterpart at Port au Port (16.5 ± 1.6 eq wt% NaCl, n ¼ 8). On the other hand, the salinity of fluid inclusions in D3 is similar at Daniel's Harbour (21.3 ± 0.6 eq wt % NaCl, n ¼ 27) and Port au Port (20.7 ± 2.7 eq wt% NaCl, n ¼ 10) but higher relative to its counterpart at Port au Choix (14 ± 1.8 eq wt% NaCl, n ¼ 11, Conliffe et al., 2012). Fluid inclusions in calcite C3 have a higher mean T_h but lower salinity at Port au Port relative to Port au Choix (116 °C, 13.7 ± 4.2 eq wt% NaCl and 102 °C, 23.6 ± 1.1 eq wt% NaCl, respectively, Table 1).

4.3. Major and trace elements

Table 2 summarizes the major and trace element concentrations of the Catoche carbonates at Daniel's Harbour and other locations across western Newfoundland. Elemental geochemical data for calcite C2 was excluded because C2 is rare and found only mixed with calcite C1, such that it was impossible to micro sample without cross contamination. The results indicate that D1 and D2 are less calcitic on the Northern Peninsula at Daniels Harbour ($CaCO_3$; D1 ¼ 51.6 ± 2%, n ¼ 15, D2 ¼ 51.9 ± 2%, n ¼ 35) and Port au Choix ($CaCO_3$; D1 ¼ 57.9 ± 2%, n ¼ 13, D2 ¼ 55.6 ± 1%, n ¼ 20), compared to their counterparts at Port au Port (D1 ¼ 60.9 ± 5%, n ¼ 5 and D2 ¼ 61.7 ± 2%, n ¼ 11). Also, the Northern Peninsula sections have a lower mean Sr concentration (Daniel's Harbour; D1 ¼ 47.3 ± 2.5 ppm, n ¼ 15 and D2 ¼ 36.4 ± 8 ppm, n ¼ 35, Port au Choix; D1 ¼ 70 ± 43 ppm, n ¼ 13 and D2 ¼ 31 ± 4 ppm, n ¼ 20) relative to their counterparts at Port au Port (D1 ¼ 106 ± 60 ppm, n ¼ 5 and D2 ¼ 68 ± 21 ppm, n ¼ 11). Dolomite D2 generally has similar Fe concentration at all locations although it is slightly enriched on the Northern Peninsula relative to those at Port au Port whereas the mean Mn concentration is lower in carbonates of the former locality (Conliffe et al., 2012).

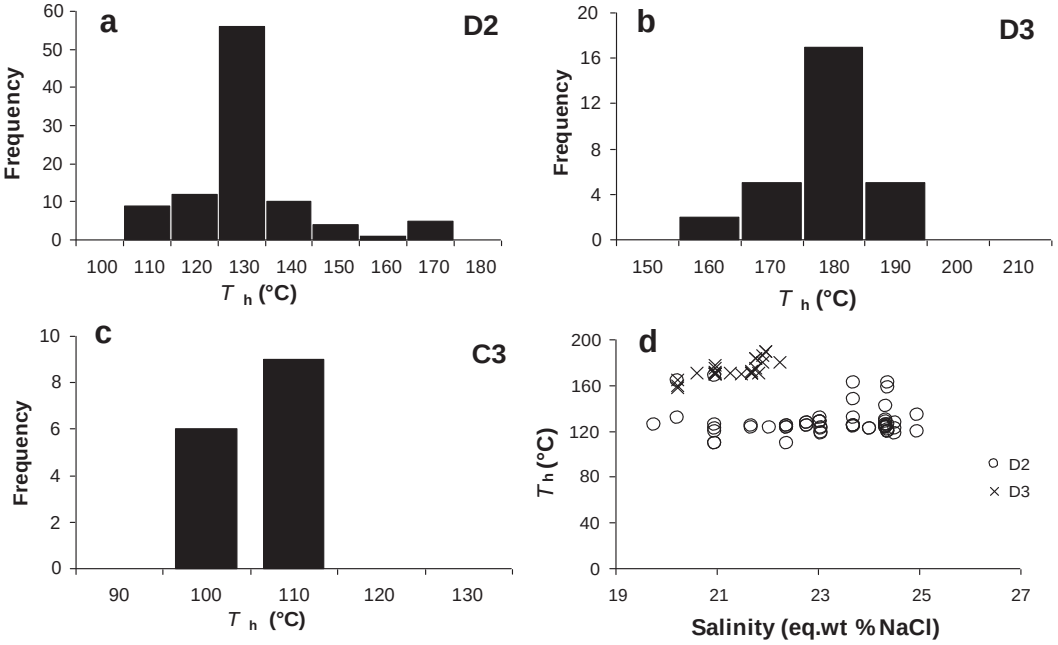

Figure 4. Plots of the microthermometric data from primary two-phase fluid inclusions trapped in D2, D3 and C3 of the Catoche Formation at Daniels Harbour showing (a) Histogram of homogenization temperature of D2, (b) Histogram of homogenization temperature of D3, (c) Histogram of homogenization temperature of C3, and (d) Scatter diagram of estimated salinity (Bodnar, 2003) vs. homogenization temperature of D2 and D3.

Table 2
$CaCO_3$, $MgCO_3$, Mn, Sr, Fe, $\delta^{18}O$ and $\delta^{13}C$ statistics for Catoche Formation carbonates in the investigated core section at Daniels Harbour and equivalent sections at Port au Choix and Port au Port (Conliffe et al., 2012).

Phase		$CaCO_3$%	$MgCO_3$%	Fe (ppm)	Mn (ppm)	Sr (ppm)	$\delta^{18}O$& (VPDB)	$\delta^{13}C$& (VPDB)
Daniels Harbour (Northern Peninsula)								
C1	n	8	8	8	8	8	8	8
	Mean	98	2	114	18	271	−9.3	−0.5
	S.D.	2	2	43	5	26	0.3	0.3
	Max	99.2	6.7	214	27	303	−8.7	−0.03
	Min	93.3	0.8	73	13	222	−9.7	−0.99
C3	n	1	1	1	1	1	4	4
	Value	95	5	205	149	17	−9.6	−3.7
	S.D.						0.2	0.9
	Max						−9.3	−2.8
	Min						−10	−4.8
D1	n	15	15	15	15	15	17	17
	Mean	51.6	48.4	1445	103	47	−9.0	−1.3
	S.D.	2	2	695	28	25	1	0.4
	Max	55.2	50.6	3082	141	126	−6.8	−0.3
	Min	49.4	46.5	720	47	26	−10.4	−2
D2	n	35	35	35	35	35	52	52
	Mean	51.9	48.1	1684	131	36	−9.5	−1.4
	S.D.	2	2	1096	50	8	0.8	0.4
	Max	57.7	50.5	4493	342	52	−7.9	−0.04
	Min	49.5	42.3	531	43	27	−11.6	−2
D3	n	12	12	11	12	12	15	15
	Mean	51.9	48.1	1784	198	39	−10.5	−1.7
	S.D.	1	1	618	55	9	1.3	0.4
	Max	53.7	49.6	3299	280	57	−7.9	−1.3
	Min	50.4	46.3	810	97	26	−13.2	−2.8
Port au Choix (Northern Peninsula)								
C1	n	13	13	13	13	13	13	13
	Mean	97.3	2.7	1607	53	362	−8.5	−1.7
	S.D.	2	2	626	17	61	0.6	0.5
	Max	98.8	6.1	2874	79	482	−7.9	−1.1
	Min	93.9	1.2	822	36	290	−9.7	−2.7
D1	n	13	13	13	13	13	13	13
	Mean	57.9	42.1	4001	100	70	−8.7	−0.8
	S.D.	2	2	1939	40	43	1.3	0.5
	Max	62.1	45	7389	183	161	−6.6	0.1
	Min	55	38	1721	56	31	−10.3	−1.7
D2	n	20	20	20	20	20	20	20
	Mean	55.6	44.4	1751	178	31	−9.2	−0.9
	S.D.	1	1	1008	90	4	1.2	0.4
	Max	57	46.5	5600	435	40	−6.9	−0.2
	Min	53.5	43	853	62	26	−10.7	−1.4
D3	n	4	4	4	4	4	4	4
	Mean	60.9	39.1	14,934	316	64	−7.3	−1.2
	S.D.	2	2	10,287	115	13	1	0.4
	Max	63.8	40.6	29,279	485	83	−6.1	−0.7
	Min	59.5	36.2	4881	240	52	−8.5	−1.5
Port au Port Peninsula								
C1	n	5	5	5	5	5	14	14
	Mean	99.4	0.6	394	98	211	−7.9	−0.7
	S.D.	0.4	0.4	253	158	166	0.6	0.5
	Max	99.7	1.2	777	379	486	−6.9	−0.1
	Min	98.8	0.3	174	15	84	−8.7	−2.2
C3	n	8	8	8	8	8	15	15
	Mean	99.1	0.9	402	798	122	−8.4	−2.6
	S.D.	1	1	244	963	87	2.4	2.4
	Max	99.8	3.2	813	2282	303	−2.3	0.4
	Min	96.8	0.2	109	11	41	−11.8	−7.4
D1	n	5	5	5	5	5	5	5
	Mean	60.9	39.1	1706	140	106	−6.1	−0.7
	S.D.	5	5	465	114	60	0.7	0.2
	Max	66	44.8	2248	342	206	−5.4	−0.5
	Min	55.2	34	1175	67	61	−6.9	−1
D2	n	11	11	11	11	11	26	26
	Mean	61.7	38.3	1589	209	68	−7	−0.8
	S.D.	2	2	1001	190	21	0.5	0.3
	Max	63.7	41.5	3354	741	108	−5.7	−0.4
	Min	58.5	36.3	490	60	46	−7.8	−1.4
D3	n	1	1	1	1	1	1	1
	Value	63	37	1178	186	65	−7.5	−0.8
	S.D.							
	Max							

4.4. Carbon and oxygen isotopes

Table 2 summarizes the isotopic composition of Catoche Formation carbonates at Daniel's Harbour and other locations in western Newfoundland. At Daniel's Harbour, mean $\delta^{13}C$ values decreased from −0.5& ± 0.3 VPDB in calcite C1 to −3.7& ± 0.9 VPDB in C3 but there is no significant change in the mean $\delta^{18}O$ values of the calcites. On the contrary, the mean $\delta^{13}C$ and $\delta^{18}O$ values of the dolomites exhibit no strong trends (Fig. 5; Table 2). Catoche dolomites at Port au Port are slightly enriched in their $\delta^{13}C$ and $\delta^{18}O$ values (Conliffe et al., 2012) relative to their counterparts on the Northern Peninsula (Table 2). No significant correlation was found between the Mn/Sr ratios and the $\delta^{13}C$ values of the dolomites in the Daniel's Harbour section (Fig. 6aec) as well at the Port au Choix and Port au Port sections (Conliffe et al., 2012).

4.5. Rare earth elements (REE)

Table 3 is the summary statistics of the REE concentrations of Arenig seawater and Catoche carbonates at Daniel's Harbour (Appendix 1), whereas Figure 8 is the corresponding shale normalized profiles. Mean SREE values are lowest in calcite C1 (5.4 ± 1.1 ppm, n ¼ 8), invariable between dolomite D1 (11.9 ± 4.8 ppm, n ¼ 15) and D2 (10.6 ± 3.9 ppm, n ¼ 35) but increased in dolomite D3 (20.7 ± 16.4 ppm, n ¼ 12) to the highest mean value.

Table 4 summarizes the statistics of the Ce and Eu anomaly calculations (Bau and Dulski, 1996). Calcite C1 has the lowest mean Ce anomaly with a value of 0.68 ± 0.06, whereas dolomite D3 has

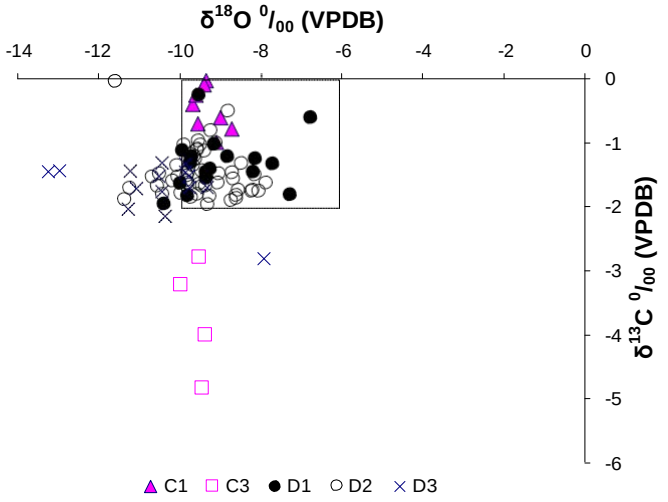

Figure 5. Scatter diagram of $\delta^{18}O$ vs. $\delta^{13}C$ for the different Catoche carbonate phases. The square represents the range of isotopic composition of best preserved carbonates precipitated from the Arenig seawater (cf. Veizer et al., 1999; Shields et al., 2003).

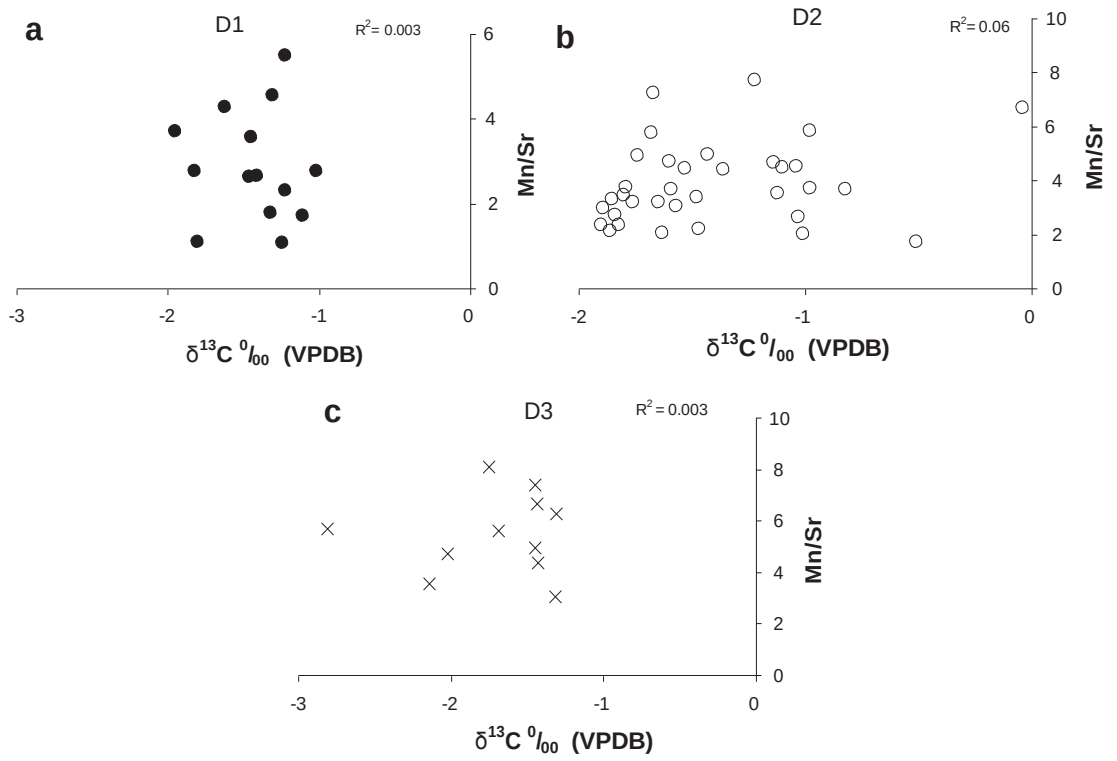

Figure 6. Scatter diagrams of $\delta^{13}C$ vs. Mn/Sr for (a) D1, (b) D2, and (c) D3 dolomites of the Catoche Formation in the investigated core section showing insignificant correlations.

the highest mean Ce anomaly with a value of 0.88 ± 0.06. Mean Ce anomaly values for all the other carbonates fall between these values. A narrow mean Eu anomaly range is displayed by the carbonates of the Catoche Formation, which range from 0.67 ± 0.08 in C1 to 0.70 ± 0.11 in D3.

4.6. Fluid-inclusion gas analysis

Results of fluid inclusion gas analysis which displays the burst weighted averages of all analysis carried out on Catoche carbonates at Daniels Harbour are as shown in Appendix 3. The weighted mean

Table 3
Summary of rare earth element concentration of Catoche carbonates at Daniel's Harbour.

Phase		La (ppb)	Ce (ppb)	Pr (ppb)	Nd (ppb)	Sm (ppb)	Eu (ppb)	Gd (ppb)	Tb (ppb)	Dy (ppb)	Ho (ppb)	Er (ppb)	Tm (ppb)	Yb (ppb)	Lu (ppb)	SREE (ppm)
D1	n	15	15	15	15	15	15	15	15	15	15	15	15	15	15	15
	Mean	2476	4900	599	2268	412	88	436	57	298	56	171	22	135	20	12
	S.D.	973	2071	248	925	169	34	157	22	106	21	61	8	45	8	5
	Max	4597	9456	1156	4373	769	158	736	97	524	102	280	38	223	38	22
	Min	1438	2562	340	1285	222	47	233	26	140	22	81	9	67	8	7
D2	n	35	35	35	35	35	35	35	35	35	35	35	35	35	35	35
	Mean	2299	4244	525	2001	367	78	377	54	282	55	161	21	131	19	11
	S.D.	837	1769	206	755	127	26	129	17	90	17	52	6	41	7	4
	Max	4452	8127	955	3654	648	127	750	102	522	102	301	35	247	36	20
	Min	1204	2020	241	1062	203	42	218	34	168	25	89	9	69	8	6
D3	n	12	12	12	12	12	12	12	12	12	12	12	12	12	12	12
	Mean	3858	8985	1137	4224	724	163	699	85	380	67	190	23	136	22	21
	S.D.	2733	7514	971	3577	572	101	518	56	212	35	96	12	65	9	16
	Max	10,269	26,917	3491	12,991	2049	344	1909	210	775	129	357	48	261	37	60
	Min	1276	2476	307	1113	202	55	202	33	166	25	73	7	42	8	6
CI	n	8	8	8	8	8	8	8	8	8	8	8	8	8	8	8
	Mean	1280	1821	248	1003	201	45	231	34	196	42	124	18	105	16	5
	S.D.	242	360	58	214	52	12	58	9	56	14	31	5	36	4	1
	Max	1692	2418	350	1354	297	66	326	49	289	68	178	25	158	24	7
	Min	917	1233	164	708	155	29	174	24	136	26	89	10	66	11	4
C3	n	1	1	1	1	1	1	1	1	1	1	1	1	1	1	1
	Value	6889	11,276	1256	4534	632	137	644	68	295	56	180	24	183	25	26
Arenig seawater (brach shells)	n	4	4	4	4	4	4	4	4	4	4	4	4	4	4	4
	Mean	362	812	100	373	57	14	61	5	27	5	16	2	15	1	2
	S.D.	151	256	34	135	20	6	27	3	9	2	9	2	10	2	1
	Max	545	1025	138	557	85	19	98	9	39	8	27	5	25	4	3
	Min	202	506	63	234	42	7	38	3	19	3	8	0.3	4	0.3	1

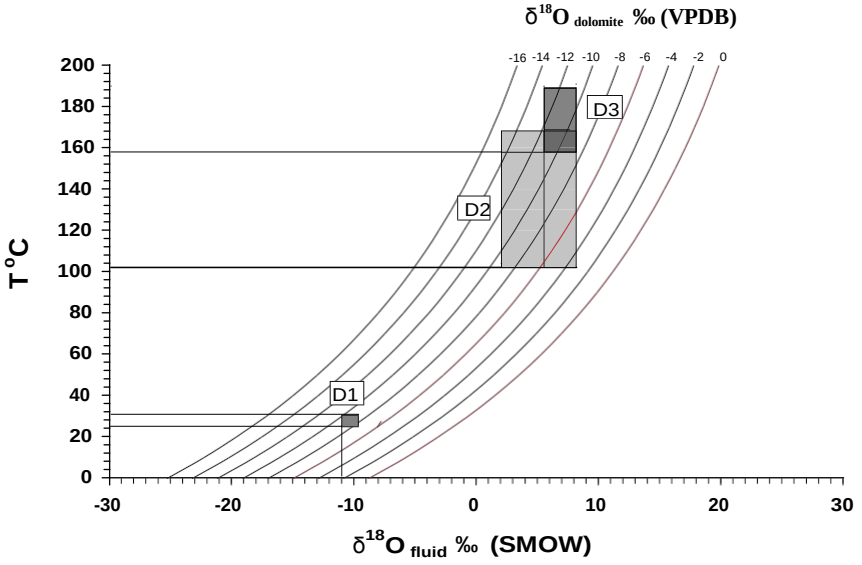

Figure 7. Temperature (T) vs. $\delta^{18}O_{dagenetic\ fluid}$ for various $\delta^{18}O_{dolomite}$ values that were reconstructed from the following equation: $10^3 \ln \alpha = 3.2*10^6 T^{-2} - 3.3$ (Land, 1983). The vertical bars indicate the ranges or $\delta^{18}O$ fluid based on the ranges of $\delta^{18}O$ values and homogenization temperature (T_h) of each identified dolomite phase.

ratio of CO_2/CH_4 varied from 0.03 to 0.08 in calcite C1, 0.10 to 0.32 in D1, 0.07 to 0.14 in D2 and 0.58 to 1.36 in D3, while the corresponding weighted mean ratio of N_2/Ar varied from 132.4 to 143.2, 80.1 to 103, 90.9 to 105.5 and 54.4 to 66.2, respectively.

5. Discussion of origin of dolomite

5.1. Dolomite petrography

The fine crystalline fabric-retentive nature and dull cathodoluminescence of the dolomicrite (D1) suggest early dolomitization of marine limemud at near-surface conditions in shallow burial settings prior to significant compaction. This is consistent with the presence of microstylolites that cut through D1 and the occurrence of D1 as dolomicrite intraclasts directly above the St. George unconformity (Lane, 1990). The very low porosity associated with D1 (<1%) suggests that dolomitization was extensive and occurred likely under open system conditions with an abundant supply of dolomite-saturated fluids, such that pores were occluded with dolomite. This agrees with the suggested origin for D1 in the Catoche Formation at Port au Choix and Port au Port (Greene, 2008; Conliffe et al., 2012).

The fabric destructive nature and larger crystal sizes of D2 (70 mme1 mm), compared with D1 (dolomicrite), suggest a later stage of replacive dolomitization that likely started with increased temperature and pressure (Warren, 2000). The cloudy core with clear rims of D2 crystals indicate replacement of a precursor carbonate (cloudy core) and cementation (clear rim) whereas zoned CL images reflect chemical variations within the crystal (Warren, 2000). Undulose extinction in dolomites is caused by distorted crystal lattice that results from crystal growth at high temperatures (e.g., Warren, 2000; Rameil, 2008; Kırmacı, 2008). This is consistent with the mean T_h (126.6 ± 12.8 °C, n ¼ 97) value of D2 and suggests crystallization at higher temperatures and deeper burial conditions relative to D1. The formation of distorted dolomite crystal lattice has also been linked to sulphate reduction (Radke and Mathis, 1980), however no evidence was found in this study

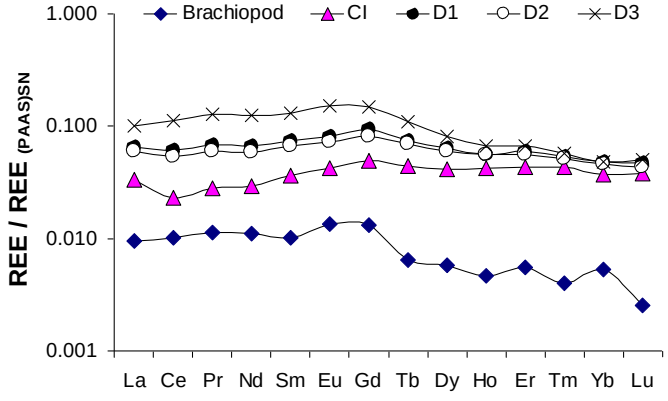

Figure 8. Mean shale-normalized (PAAS) values of REE concentrations of best preserved Arenig brachiopod shells and the respective phases of Catoche carbonates. Details in text.

Table 4
Summary statistics of Ce $(Ce/Ce^*)_{SN}$ and Eu $(Eu/Eu^*)_{CN}$ anomaly analysis of Catoche carbonates at Daniel's Harbour based on the equations by Bau and Dulski (1996).

Phase		Ce^*_{SN} anomaly	Eu^*_{CN} anomaly
C1	n	8	8
	Mean	0.68	0.67
	S.D.	0.06	0.08
	Max	0.76	0.76
	Min	0.60	0.52
D1	n	15	15
	Mean	0.85	0.67
	S.D.	0.05	0.05
	Max	0.94	0.79
	Min	0.77	0.59
D2	n	35	35
	Mean	0.81	0.65
	S.D.	0.06	0.05
	Max	0.91	0.75
	Min	0.70	0.56
D3	n	12	11
	Mean	0.88	0.70
	S.D.	0.06	0.11
	Max	0.96	0.88
	Min	0.76	0.50

to support the occurrence of either bacterial sulphate reduction (BSR) or thermochemical sulphate reduction (TSR) in the Catoche Formation at the current study locations, although Mississippi valley type leadezinc sulphide ores have been discovered and mined north of Daniel's Harbour (Lane, 1990). The generally higher mean T_h measurements from Catoche dolomites on the Northern peninsula relative to its counterparts on the Port au Port, may reflect relatively deeper settings for the former location (Table 1). The high intercrystalline porosity associated with D2 indicates dolomitization under a closed to semi-closed system with lower watererock ratio (compared to D1) and limited external supply of $Mg^{2þ}$ ions such that no extra dolomite occluded the developed intercrystalline pores. Some of these pores are filled with bituminous material that exhibits a blue fluorescence in UV light (Fig. 3i, j). The fluorescence hue and spectra (profile) of the bituminous material is identical to that of known crude oil samples from Jeanne d'Arc basin, off the coast of eastern Newfoundland (e.g., Roedder, 1984; Gillespie and Burden, 2010) and likely suggests the occurrence of hydrocarbon in the formation.

The mean T_h of D3 (174.1 ± 7.6 °C, n ¼ 29), coupled with its limited distribution, imply development at the very late stages of diagenesis at higher temperature relative to D2. The generally higher mean T_h values for dolomites on the Northern Peninsula suggest relatively deeper burial to the Port au Port Peninsula section (Table 1).

Despite the difference in the ranges of T_h values, the considerable overlap in the salinity and measured T_h values of fluid inclusions associated with D2 and D3 (Fig. 4a, b and d; Table 2) suggests that they likely formed from fluids of similar composition but at different temperatures in a closed system or possibly from the same fluids that circulated during burial in a close to semi-closed system. This is consistent with the occurrence of intercrystalline pores in D3 similar to those commonly associated with D2. A similar overlap in salinity and T_h was documented by Conliffe et al. (2012) in dolomites at Port au Choix and Port au Port. The mean salinity and T_h values of fluid inclusions associated with D2 and D3 at Daniel's Harbour (Table 1), are high and 5e10 °C greater than the maximum burial temperature of the Catoche Formation at this locality (115e120 °C). This implies that both generations of dolomite are hydrothermal.

5.2. Major and trace elements

The mean values of $CaCO_3$ and $MgCO_3$ concentrations of D1 at Daniel's Harbour (Table 2) indicate near-stoichiometric dolomite (Appendix 1) with mean Sr concentration of 47 ± 25 ppm (<550 ppm; Tucker and Wright, 1990). This suggests a coeval open system with an abundant supply of Mg ions or alteration of a precursor Mg-rich polymorph of $CaCO_3$ in an open system (e.g., Sperber et al., 1984; Azmy et al., 2001, 2008) rather than a hypersaline sabkha origin (Lane, 1990). This is consistent with the absence of evaporite beds in the Catoche and surrounding formations (cf. Meyers et al., 1997; Lu and Meyers, 1998; Azmy et al., 2001, 2008) and lack of moldic porosity within the Catoche Formation (Land, 1967; Matthews, 1974; Longman, 1980; James and Choquette, 1984; Moore, 1997). Consistency in near stoichiometry and narrow ranges of Sr, Mn, and Fe variations in dolomites D1 to D3 (Table 2) probably reflects localized circulation of fluids of similar compositions through crustal rocks, which got hotter with subsequent dolomitization events during diagenesis. The occurrence of non-stoichiometric calcian dolomite at Port au Choix and Port au Port suggests possibly less fluid mobility and/or a relatively limited supply of $Mg^{2þ}$ (e.g., Sperber et al., 1984).

Iron (Fe) and Manganese (Mn) concentrations are indicators of redox conditions during dolomitization. The general increase in the mean values of Fe and Mn concentrations from calcite C1 to C3 and D1 to D3 at Daniel's Harbour (Table 2) reflects a decrease in oxidizing conditions from the earliest dolomite generation (D1) to the latest generation (D3). The relatively higher Fe content of D1 at Port au Choix, compared with other locations, is probably due to the influence of terrestrially derived fluids (riverine input) rather than reducing conditions since most petrographic and geochemical evidences support formation at or near the surface (Greene, 2008; Conliffe et al., 2012). The slightly higher Fe content of D2 dolomite on the Northern Peninsula suggests reduced oxidizing conditions consistent with deeper burial settings and higher T_h values (Table 1).

Although it has different petrographic features, D3 at Daniel's Harbour is geochemically similar to D2 (Table 2). This may suggest that both D2 and D3 formed from similar or the same diagenetic fluids but at different temperatures, which supports the overlap in their salinity and T_h values (Table 1). A similar feature has been documented at Port au Port and is akin to non-saddle and saddle D2 dolomite at Port aux Choix (Table 2; Conliffe et al., 2012).

5.3. Carbon and oxygen isotopes

The $\delta^{13}C$ and $\delta^{18}O$ values of C1 and most of D1, are within range of values of the best preserved carbonates precipitated from Arenig seawater (Fig. 5), suggesting a high degree of preservation of its primary isotopic signatures particularly those of carbon (cf. Veizer et al., 1999; Shields et al., 2003). This is supported by the lack of correlation between Mn/Sr and $\delta^{13}C$ values (Fig. 6). The overlap ranges in $\delta^{13}C$ values of dolomites D1 and D2 with those of calcite C1 suggests that C1 was likely the precursor for these dolomite generations as diagenetic fluids generally have low dissolved CO_2 (low pCO_2; Land, 1992), which makes resetting of C-isotope signatures difficult in many cases. Also, the considerable overlap in the $\delta^{13}C$ signature of dolomites D2 and D3 coupled with the lack of correlation between Mn/Sr and $\delta^{13}C$ in all generations of dolomite (Figs. 5 and 6), implies that deposition of the bituminous material, sometimes occluding intercrystalline pores associated with D2, occurred after D2 but prior to D3 rather than contemporaneous with either dolomite precipitation, i.e. dolomitization was not influenced by carbon from organic matter. The variations in the mean $\delta^{13}C$ and $\delta^{18}O$ values of Catoche dolomites at Daniel's Harbour are consistent with diagenetically closed or semi-closed system conditions. The significant overlap in $\delta^{18}O$ values of dolomites D1 to D3 with many values of the best preserved carbonates precipitated from Arenig seawater (Fig. 5), suggests that dolomitizing fluids might have originated from modified Arenigian or slightly older seawater.

Dolomitization requires a large supply of Mg-rich fluids such as seawater. Thus, the isotopic composition of oxygen in dolomites is ultimately influenced by that of the dolomitizing fluid and the temperature of dolomitization (Land, 1992). Therefore, the $\delta^{18}O$ composition of dolomitizing fluids can be determined, if the temperature of dolomitization is known (Land, 1983). Homogenization temperatures of primary liquidevapour fluid inclusions, nature of rock fabric and fossil content can be used as proxies for temperature of dolomitization (Goldstein and Reynolds, 1994). The fabric-retentive texture of D1 coupled with the near-micritic grain size and occurrence of fenestral and stromatolitic lime mudstones (Knight et al., 2007) along with the absence of evaporite interbeds in the Catoche Formation, reflect warm (w20 °C), possibly humid, tropical conditions similar to present-day ones. The best preserved $\delta^{18}O$ values of carbonates (low-Mg calcite brachiopod shells), that precipitated from Arenig seawater during the time of deposition of the Catoche Formation are between −8.2 and −10.1‰ (VPDB; Shields et al., 2003; Bassett et al., 2007). This may reflect

precipitation from tropical seawater with a mean $\delta^{18}O$ value of ~−7.2‰ (SMOW) and values between approximately −6.2 to −8.2‰ (SMOW) at 20 °C (Hayes and Grossman, 1991). The dolomicritic crystal size suggests that D1 (the earliest dolomite), was formed during an early stage of diagenesis at near-surface conditions (temperatures ~25e30 °C, cf. Goldstein and Reynolds, 1994). Therefore, the $\delta^{18}O$ signatures of D1 at Daniel's Harbour (−9.02 ± 1‰ (VPDB), n ¼ 17. Table 2) suggest that $\delta^{18}O$ values of the dolomitizing fluid were approximately between −10 and −11.2‰ (VSMOW) with a mean of about −10.6‰ (VSMOW; Fig. 7; Shields et al., 2003; Bassett et al., 2007). The difference between the average $\delta^{18}O$ compositions of seawater and meteoric waters in modern tropical environment is ~4‰ (SMOW, Clark and Fritz, 1997). Assuming that the difference in $\delta^{18}O$ compositions between the Arenig meteoric and seawaters was similar to that of the modern environment, the mean $\delta^{18}O$ value of Arenig meteoric water would be −11.2‰ (SMOW) (i.e. ~ 4‰ lower than −7.2‰). Thus, the estimated $\delta^{18}O$ values of the dolomitizing fluids which formed D1 falls within the calculated mean range of Arenig meteoric (−11.2‰, SMOW) and seawater (−7.2‰, SMOW). This suggests that the earliest dolomite originated from modified seawater i.e. Arenig seawater slightly diluted with Arenig meteoric water (e.g., Azmy et al., 2009; Greene, 2008; Conliffe et al., 2012), which is consistent with the low Sr and high Fe contents coupled with the lack of evaporite beds in the Catoche Formation. Applying the above approach at the same temperature to D1 at Port au Choix (Greene, 2008) and Port au Port (Conliffe et al., 2012), suggests that $\delta^{18}O$ value of fluids that precipitated D1 varied from −9.7 to −10.8‰ (VSMOW) and −7 to −8.2‰ (VSMOW), respectively. Thus, the dolomitizing fluids for D1 were more enriched in ^{18}O on the Port au Port peninsula relative to the Northern Peninsula, which suggest that dolomitizing fluids on the Northern Peninsula had a higher Arenig meteoric water content compared to their counterpart on the Port au Port Peninsula (Conliffe et al., 2012). This is consistent with lower Sr and higher Fe concentrations of D1 on the Northern Peninsula (Table 2; Appendix 1). On the other hand, the estimated $\delta^{18}O$ composition of dolomitizing fluids for dolomites D2 and D3 in the Daniel Harbour section is more enriched (þ2.1 to þ8.1‰ and þ5.8 to þ8.1‰, VSMOW respectively) relative to D1 dolomitizing fluids (Fig. 7), which is normal for fluids formed at higher temperatures with deeper burial. Deep-basinal brines are usually highly saline and enriched in ^{18}O irrespective of age and location (Goldstein and Reynolds, 1994; Azmy et al., 2001; Lonnee and Machel, 2006). Thus, T_h and salinity measurements coupled with the $\delta^{18}O$ signatures of the dolomitizing fluids for dolomites D2 and D3 reflect a hydrothermal origin (Conliffe et al., 2010). This is also consistent with the postulated origin of dolomites D2 and D3 at Port au Choix and Port au Port (Greene, 2008; Conliffe et al., 2012). The overlap in estimated $\delta^{18}O$ values of dolomitizing fluids for dolomites D2 and D3 (Fig. 7) at the Daniel's Harbour section implies that both generations likely precipitated from similar fluids or possibly the same fluids as those of D1 that evolved by circulation through crustal rocks under closed system conditions (e.g., Azmy et al., 2009; Conliffe et al., 2012), which is also supported by the invariant mean salinity values for both dolomites D2 and D3 (Table 1). A similar overlap has been reported for dolomites D2 and D3 at Port au Choix (Greene, 2008).

The slightly lower $\delta^{13}C$ values of dolomites at Daniel's Harbour relative to their counterparts at other locations (Table 2) are most likely controlled by the precursor carbonate (C1). The higher $\delta^{13}C$ values for calcite C1 at Daniel's Harbour (−0.48‰ (VPDB) ± 0.34, n ¼ 13) and at Port au Port (−0.7‰ (VPDB) ± 0.5, n ¼ 14), compared with those at Port au Choix, is consistent with calcites that initially had a higher proportion of high magnesium calcite (Romanek et al., 1992; Swart and Eberli, 2005; Weissert et al., 2008). Generally speaking, the insignificant variations in the mean $\delta^{13}C$ values among the equivalent dolomite generations at all three locations suggest possible regional circulation of diagenetic fluids with similar compositions across western Newfoundland rather than regional mixing with magmatic fluids (e.g., Lavoie et al., 2010). The diagenetic fluids probably became hotter during circulation through crustal rocks of deeper settings.

The lack of correlation between $\delta^{13}C$ and Mn/Sr values particularly for the near-micritic and fabric retentive D1 at Daniel's Harbour (Fig. 6), implies that the $\delta^{13}C$ values are near primary and the reconstructed $\delta^{13}C$ profile (Fig. 2) is suitable for chemostratigraphic correlations (e.g., Azmy and Lavoie, 2009; Azmy and Conliffe, 2010). A similar result was reported for the Port au Choix and Port au Port sections (Greene, 2008; Conliffe et al., 2012). Figure 2 shows the $\delta^{13}C$ profile of Catoche dolomites at the three locations across western Newfoundland. The $\delta^{13}C$ profiles show a common negative shift at the top and a similar but broader one at the middle that can be utilized for refining stratigraphic correlation of the formation across the area.

5.4. Rare earth elements (REE)

The suite of rare earth elements (REE) is a useful tool for the identification of the origin of fluids, the state of equilibrium in rocke water interactions and changes in fluid composition, which is fundamental in understanding fluid-rock systems. The suite consists of fifteen lanthanides and is traditionally classified into light rare earth elements (LREE; La to Nd), medium rare earth elements (MREE: Sm to Dy) and heavy rare earth elements (HREE; Ho to Lu). REEs have relatively short residence time (several hundred years; Alibo and Nozaki, 1999) and are lithophile elements that invariably occur together naturally because all are trivalent (except for $Ce^{þ4}$ and $Eu^{þ2}$ in certain environments) and have similar ionic radii with chemical characteristics that change systematically along the series, which results in the preferential absorption of LREE relative to MREE and HREE in seawater (Sholkovitz and Shen, 1995). Their incorporation into calcite (biogenic and abiogenic) lies within a relatively narrow range of partition coefficient values (Zhong and Mucci, 1995), and thus observed variation in the series is a reflection of oceanic composition and/or nature of fluids that deposited the carbonates and other processes. Redox conditions control the conversion and distribution of Cerium (Ce) and to a lesser degree Europium (Eu) (Sholkovitz et al., 1994); hence both elements provide further information on process controlling parameters. The earlier concept that limestone was a poor choice for seawater REE proxy due to the effects of diagenesis in ancient carbonates (e.g., Scherer and Seitz, 1980; Shaw and Wasserburg, 1985), was replaced by the current paradigm, which suggests that diagenesis, particularly meteoric and mixed water, has no effect on the pattern, composition and/or distribution of REEs in carbonates (limestones and dolomites) except in diagenetic systems with extremely large watere rock ratios (e.g., Banner et al., 1988; Barton et al., 2006; Webb and Kamber, 2000; Kamber and Webb, 2001; Nothdurft et al., 2004; Webb et al., 2009).

Using the mean REE concentrations (Table 3) and shale normalized (REE_{SN}) values of the best preserved brachiopods (low-Mg calcite) precipitated during the Arenig as a proxy for Arenig seawater (Azmy et al., 2011), a plot of the mean shale normalized (REE/REE_{SN}) values for Catoche carbonates and Arenig seawater is shown in Figure 8. Limemud (calcite C1) and dolomite D1 have similar and parallel profiles that generally mimic those of the Arenig well preserved low-Mg calcite brachiopod shells, whereas the profiles of D2 and D3 are identical and show a slight depletion in HREE compared to MREE. This trend suggests that the REE

composition of diagenetic dolomites is at least partially controlled by that of the precursor carbonate and that the parent fluids which precipitated dolomite D1 likely contained Arenig seawater. Identical profiles with depleted HREE relative to MREE in D2 and D3, suggests that the same hydrothermal fluids precipitated both dolomite generations but at different temperatures and burial settings. The pattern for calcite C1 shows enrichment in total REE contents (5 ± 1 ppm, n ¼ 8) relative to that of the brachiopods (2 ± 1 ppm, n ¼ 4). This reflects the influence of alteration despite the petrographic preservation of micritic grain size and fabric. However, it is noteworthy that despite the reset in the REE composition, calcite C1 may retain its near-primary $\delta^{13}C$ signature due to the low pCO_2 in diagenetic fluids. The micritic grain size of C1 suggests that alteration occurred in near-surface conditions (i.e. in an oxidizing environment), which is consistent with its negative Ce anomaly (Figs. 8, 9a and Table 4). The similarities between calcite C1 and dolomite D1 in their shale normalized REE profiles (Fig. 8), $\delta^{13}C$ signatures (Fig. 5), SREE contents (Table 3) and fabric preservation coupled with <550 ppm Sr concentrations for D1 (Table 2), are strong evidence of support for calcite C1 as the precursor for dolomite D1 and thus, the Catoche dolomicrites are not syngenetic and therefore cannot be hypersaline sabkha dolomites as was previously believed (e.g., Lane, 1990). Also, the occurrence of REE normalized pattern of calcite C1 between those of the Arenigian well-preserved (low-Mg calcite) brachiopods (lower) and the dolomicrite (upper) supports the scenario of deposition of D1 at very early stage of diagenesis from solutions that were likely a mixture of Arenig meteoric and marine waters.

Ce and La anomalies of the Catoche dolomites and calcite C1 cluster around unity (Fig. 9), which suggests that they were diagenetically altered in REE equilibrium with their respective diagenetic fluids (Fig. 8). Hence, observed variations in REE_{SN} and SREE of the respective carbonate phases reflect evolution of fluid composition during diagenesis. Furthermore, La anomaly is minor whereas Ce anomaly is mostly negative (Fig. 9). The normalized REE patterns of Catoche dolomites (Fig. 8), coupled with insignificant variations in their respective SREE contents (Table 3), strongly supports the suggested scenario of mixed waters as the source fluids for D1 and circulated basinal fluids of similar composition (or possibly same composition as D1) as the source fluids for D2 and D3 and excludes the involvement of magmatic fluids or fluids of other origins in dolomitization (e.g., Azmy et al., 2008, 2009, 2011; Azmy and Conliffe, 2010; Conliffe et al., 2010; Lavoie et al., 2010).

All Ce anomaly values (Table 4) suggest oxic to suboxic fluid conditions during the formation/diagenesis of Catoche dolomites and calcite C1 whereas Eu anomalies expressed as $(Eu/Eu^*)_{CN,}$ are consistent with low temperatures (<250 ^{0}C) for the diagenetic fluids that precipitated the dolomites and calcite (e.g., Möller, 2000; Wilde et al., 1996; Bau and Dulski, 1996), which is supported by petrographic features, elemental compositions and fluid inclusion analyses of the respective carbonates. Calculated Eu anomalies coupled with fluid inclusion analysis of Catoche dolomites D2 and D3 and calcite C3, strongly suggest that temperature(s) of dolomitization and latest calcite precipitation was <200 ^{0}C as positive Eu anomaly only occurs at temperatures above 250 ^{0}C (Bau and Dulski, 1996; Möller, 2000), which supports the exclusion of magmatic fluids.

5.5. Fluid inclusion gas analyses

Analysis of gases trapped in fluid inclusions provides yet an additional tool to ascertain the oxidation state and discriminate the origin of source fluids in geologic systems. Giggenbach (1986) introduced the concept that N_2eAreHe ratios of geothermal gases may identify the source of volatiles in geothermal fluids. Norman and Moore (1999) introduced the use of methane (i.e. ratio of N_2eAreCH$_4$) as a tracer species because; CH_4 provides an indication of the crustal component in thermal fluids; there is no

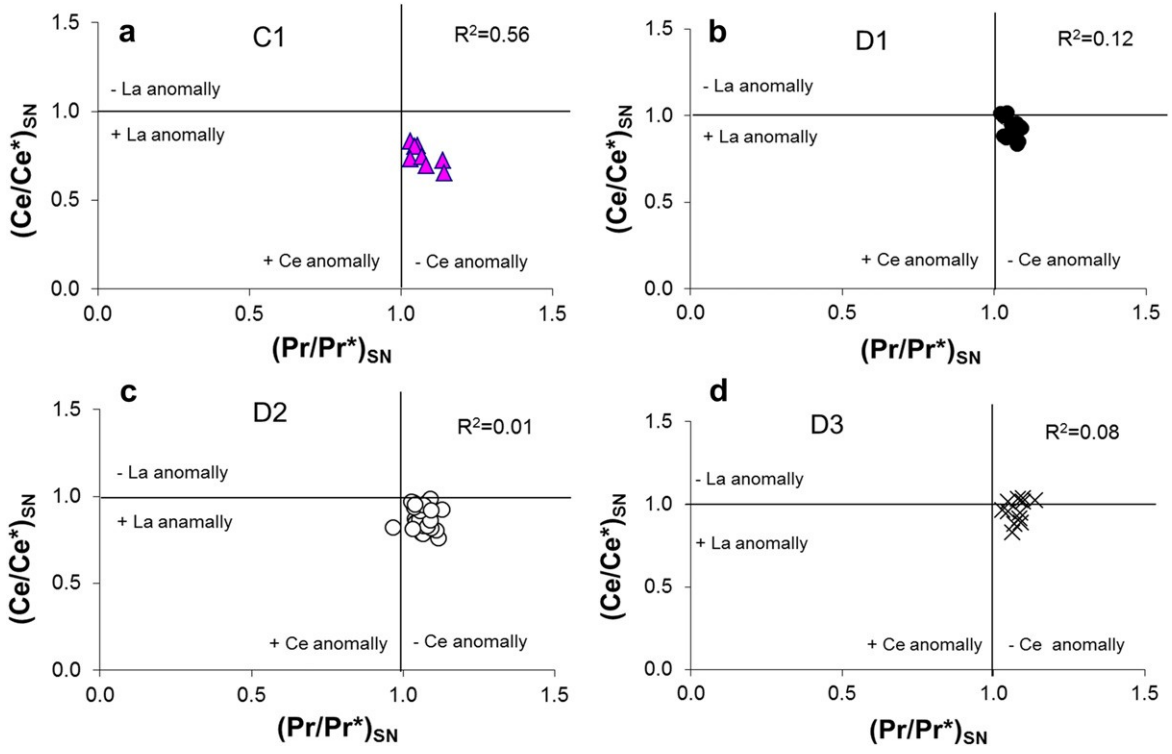

Figure 9. Ce and La anomalies (La ¼ $(Pr/Pr^*)_{SN}$) plots for (a) C1, (b) D1, (c) D2, and (d) D3. The values, with few exceptions, cluster close to the unity lines. Details in text.

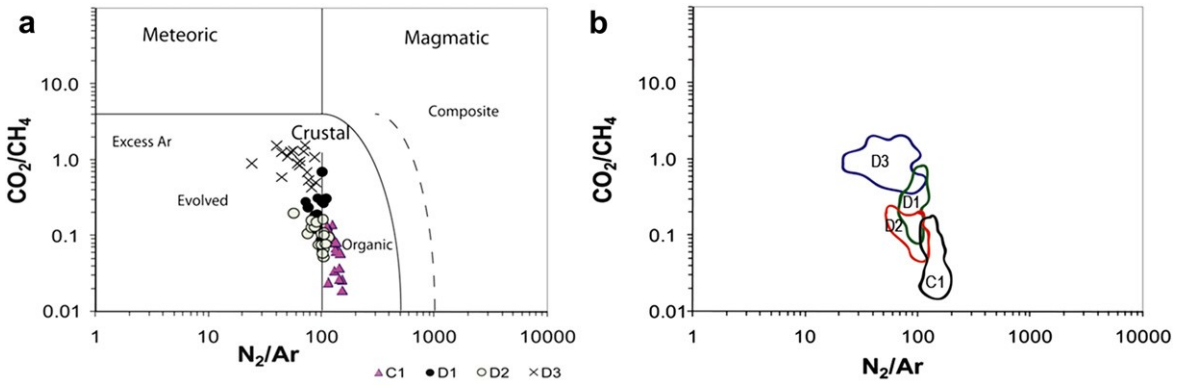

Figure 10. Plots of gas analysis of Catoche Formation fluid inclusion gases showing (a) Scatter diagram of CO_2/CH_4 vs. N_2/Ar, and (b) Data fields for the respective Catoche carbonates showing overlap.

ambiguity about the origin of methane as there is with helium and it is easier to analyse. Norman and Moore (1999) also introduced the concept of CO_2/CH_4 versus N_2/Ar diagram that can differentiate fluids bearing significant organic nitrogen, which could lead to errors in interpretation. The CO_2/CH_4 versus N_2/Ar diagram of Norman and Moore (1999) classified source fluids into three basic groups; magmatic, meteoric and crustal fluids. Meteoric fluids refer to near-surface recharge waters while crustal fluids refer to meteoric fluids that have interacted with crustal rocks and may have species derived from the wall rock. The ratio of CO_2/CH_4 indicates the redox state while N_2/Ar provides an indication of fluid source(s).

Figure 10a, b exhibits the plots of CO_2/CH_4 against N_2/Ar ratios for Catoche carbonate inclusion gases at Daniel's Harbour. The data points plot well inside the crustal zone and preclude fluid(s) of a magmatic origin were neither present in the Catoche carbonates nor involved in the dolomitization process. Rather, Crustal (basinal) fluids which evolved from meteoric waters are present in all generations of Catoche dolomite (Fig. 10a). The evolution of meteoric waters likely occurred via mixing with seawater as meteoric waters do not have enough Mg^{2+} to cause dolomitization. Calcite C1 plots within the organic field; which implies that there is sufficient organic nitrogen to increase the N_2/Ar ratio above that of air-saturated water. This is consistent with elevated methane levels in the fluid inclusion gas analyses of C1 (Appendix 3) as nitrogen and methane are by-products of protein decay. Release of methane via organic decay also explains why source fluids associated with C1 appear to be more reduced relative to the dolomites (Fig. 10a, b). Data points of inclusion gases of dolomites D1 and D2, which plot slightly into the organics field, are likely relics of calcite C1. This suggests that calcite C1 is the precursor for these dolomites and is consistent with the overlap in their $\delta^{13}C$ values (Fig. 5), similarities in normalized REE profiles (Fig. 8) and overlap in values of inclusion gases (Fig. 10b). This indicates that D2 likely originated from the recrystallization of D1 and direct dolomitization of calcite C1.

6. Variations in porosity distribution

Porosity (ϕ) is a key parameter in reservoir characterization and plays an important role in the evolution of hydrocarbon reservoirs. Fluorescence from micro spectroscopy analyses in ultraviolet light (Fig. 3i, j), and documented occurrence of bitumen in pores associated with D2 dolomite of the Catoche Formation at other locations (e.g., Greene, 2008; Conliffe et al., 2012), refers to early emplacement of hydrocarbons prior to the precipitation of D3. The preserved porosity in the Catoche Formation is mainly secondary and occurs in dolomites (Fig. 2), suggesting that it is directly related to the dolomitization process (e.g., Dravis, 1992; Esteban and Taberner, 2003; Wierzbicki et al., 2006; Azmy et al., 2009; Conliffe et al., 2009; Azmy and Conliffe, 2010). Porosity is mostly of the intercrystalline variety (apparent long axes of pores w50e 600 mm) and mainly associated with D2 but also occasionally occurs among the subhedral crystals of D3. Dissolution vugs (up to 2.5 mm) and stylolites also occur in the formation. Some of the intercrystalline pores and vugs are filled with D3 and C3 but frequently with bituminous materials. The calcite C3 cement likely originated from late-stage non-ferroan Ca-rich fluids that were emplaced after D3. Depleted $\delta^{18}O$ values measured in calcite C3 (Table 2) are consistent with the suggested late-stage mid to deep burial origin (Azmy et al., 2009). Intercrystalline porosity likely developed during dolomitization in closed to semi-closed conditions due to the difference in molar crystal volume of dolomite compared to its precursor calcite. The decrease in volume of the resulting dolomite is thus accompanied by porosity development (Weyl, 1960; Warren, 2000); hence volume change is consistent with dolomitization of a precursor calcite while no significant volume change is expected during recrystallization of dolomicrite. If dolomitization operated under completely open system conditions, resulting pores from volume change would be occluded with dolomite cements (cf. Lucia and Major, 1994). Dissolution and the resultant vugs generally occur in response to a significant change in the chemistry of pore fluids such as changes in salinity, temperature, or partial pressure of CO_2 while stylolites develop in response to compaction pressures. Stylolites may increase the permeability of carbonates by acting as conduits for fluid transport (Moore, 1997). Petrographic and geochemical features of the Catoche D2 are similar to those documented for Rhaetian (Upper Triassic) dolomites of the Sorrento Peninsula (Southern Italy; Iannace et al., 2011).

Distribution of porosity in the Catoche Formation is controlled by the relative degree of D2 dolomitization with porosity (ϕ) varying between <1 and 12% in the Daniel's Harbour sequence. Similar porosities were observed in the Catoche carbonates at Port au Port and Port au Choix. On the Port au Port peninsula, porous horizons (estimate of ϕ ¼ 4e10%) are generally thin (<5 m) but greater than 5 m at Daniel's Harbour and Port au Choix. This suggests that D1 dolomitization was relatively more pervasive on the Port au Port Peninsula relative to Northern Peninsula (Conliffe et al., 2012), leaving only thin horizons of undolomitized limestone to be dolomitized in later stages of diagenesis and thus host intercrystalline porosity. Figure 2 shows the distribution of porosity in the Catoche Formation at all three locations. Previous studies of the Catoche dolomites reveal that porous intervals are usually

dominated by calcian D2 dolomites. This lead authors to suggest that such porous D2 horizons likely resulted from a one-step dolomitization of a precursor calcite (lime mudstones) while non-porous D2 intervals formed by recrystallization of D1 (e.g., Conliffe et al., 2012; Azmy and Conliffe, 2010; Azmy et al., 2008, 2009; Greene, 2008). Porous D2 horizons at Daniel's Harbour are slightly more calcian (mean $CaCO_3$ for porous horizons ¼ 52.2% ppm ± 2) compared with non-porous D2 horizons (mean $CaCO_3$ for non-porous horizons ¼ 50.65% ppm ± 1). The porous (f 2' 4%) horizons of the Catoche Formation at Daniel's Harbour occur in 4 layers (Fig. 2). Three are about 4 m thick, approximately 6 m, 120 m and 150 m from the top of the section whereas the fourth is about 40 m thick approximately 70 m from the top of the section. Similarly, the equivalent section at Port au Port has 4 porous intervals about 12 m, 4 m, 8 m and 8 m thick at approximately 24 m, 44 m, 48 m and 74 m respectively from the top of the section. In contrast, the porous intervals are in the first w50 m of the section at Port au Choix. This may suggest that the Catoche porous zones occur at different stratigraphic levels and are unlikely continuous across western Newfoundland, which is contrary to the reported distribution pattern of the porous zones in the underlying Watts Bight Formation (Azmy and Conliffe, 2010). However, the Catoche porous zones are characterized by broad negative $\delta^{13}C$ shifts (Fig. 2) that were likely caused by sea-level change and associated carbon cycling changes (Azmy et al., 2009; Azmy and Lavoie, 2009; Azmy and Conliffe, 2010), a common case in the carbonate sequence of the St. George Group in western Newfoundland.

7. Conclusions

Petrographic examination of the Catoche Formation carbonates from boreholes 12i/4-1 and 12i/6-121 at Daniel's Harbour on the Northern Peninsula of western Newfoundland reveals four distinct generations of dolomite, from the oldest to the youngest: replacive dolomicrite (D1), stylolite-associated dolomites (Ds), replacive and vug filling eu- to sub-hedral zoned dolomite (D2) and sub- to anhedral pore-filling saddle dolomite (D3). Dolomite D2 (with some subhedral D3) is characterized mostly by intercrystalline porosity (f < 1e12%) and zoned crystals.

Trace element and stable isotope geochemistry coupled with fluid inclusion gas analyses of the dolomites and microthermometric measurements on the trapped primary two-phase fluid inclusions, suggest that D1 formed at an early stage of diagenesis and likely from fluids consisting of a mixture of Arenig marine and meteoric waters in open system conditions. On the contrary, dolomites D2 and D3 formed at mid to deep burial settings from high temperature, high salinity fluids under suboxic conditions in closed to semi-closed system during later stages of diagenesis.

The SREE contents, shale-normalized patterns, Ce and Eu anomalies, as well as geochemical and gas inclusion analyses, reflect the evolution of the diagenetic fluids throughout the sediments burial history and support formation under oxic conditions from mixed waters (D1) and under suboxic conditions from hot non-magmatic basinal fluids that were circulated through crustal rocks (D2 and D3).

Stratigraphic levels of porous horizons in the Catoche Formation at Daniel's Harbour do not correlate with their equivalents levels in sections at Port au Choix and Port au Port (separated by w30 and 230 km, respectively), which suggests that porous zones are discontinuous across western Newfoundland, but are associated with broad negative $\delta^{13}C$ shifts. The porosity associated with D2 coupled with appropriate thermal maturation, occurrence of suitable traps, evidence of hydrocarbon accumulation as well as reported seeps containing live oil, suggests that the Catoche dolomites are potential reservoirs and suitable hydrocarbon targets.

Acknowledgements

The authors wish to thank Dr. Cathy Hollis and other reviewers for their constructive reviews. Also, efforts of Dr. Karla Bell (Journal Manager) and Dr. Nereo Preto (associate editor) are much appreciated. This project was supported by funds (to Karem Azmy) from the Petroleum Exploration Enhancement Program (PEEP).

Appendix A. Supplementary data

Supplementary data related to this article can be found online at http://dx.doi.org/10.1016/j.marpetgeo.2012.10.007.

References

Alibo, D.S., Nozaki, Y., 1999. Rare earth elements in seawater: particle association, shale normalization and Ce oxidation. Geochimica et Cosmochimica Acta 63, 363e372.

Azmy, K., Conliffe, J., 2010. Dolomitization of the lower St. George Group on the Northern Peninsula in western Newfoundland: implications for lateral distribution of porosity. Bulletin of Canadian Petroleum Geology 58 (4), 1e14.

Azmy, K., Lavoie, D., 2009. High-resolution isotope stratigraphy of the Lower Ordovician St. George Group of western Newfoundland, Canada: implications for global correlation. Canadian Journal of Earth Sciences 46, 403e423.

Azmy, K., Veizer, J., Misi, A., De Olivia, T., Dardenne, M., 2001. Isotope stratigraphy of the Neoproterozoic carbonate of Vazante Formation, Saõ Francisco Basin, Brazil. Precambrian Research 112, 303e329.

Azmy, K., Lavoie, D., Knight, I., Chi, G., 2008. Dolomitization of the Aguathuna Formation carbonates of Port au Port Peninsula in western Newfoundland, Canada: implications for a hydrocarbon reservoir. Canadian Journal of Earth Sciences 45, 795e813.

Azmy, K., Knight, I., Lavoie, D., Chi, G., 2009. Origin of the Boat Harbour Dolomites of St. George Group in western Newfoundland, Canada: implications for porosity controls. Bulletin of Canadian Petroleum Geology 57, 81e104.

Azmy, K., Brand, U., Sylvester, P., Gleeson, S.A., Logan, A., Bitner, M.A., 2011. Biogenic and abiogenic low-Mg calcite (bLMC and aLMC): evaluation of seawater-REE composition, water masses and carbonate diagenesis. Chemical Geology 280, 180e190.

Baker, D., Knight, I., 1993. The Catoche Dolomite Project, Anticosti Basin, Eastern Canada: CERR Report. Memorial University of Newfoundland, St. John's, Nfld, 174 pp.

Banner, J.L., Hanson, G.N., Meyers, W.J., 1988. Rare earth element and Nd isotopic variations in regionally extensive dolomites from the Burlingtone Keokuk Formation (Mississippian): implications for REE mobility during carbonate diagenesis. Journal of Sedimentary Petrology 58, 415e432.

Barton, E.D., Bau, M., Alexander, B., 2006. Preservation of primary REE patterns without Ce anomaly during dolomitization of Mid-Paleoproterozoic limestone and the potential re-establishment of marine anoxia immediately after the 'Great Oxidation Event'. South African Journal of Geology 109, 81e86.

Bassett, D., Macleod, K.G., Miller, J.F., Ethington, R.I., 2007. Oxygen isotopic composition of biogenic phosphate and the temperature of early Ordovician seawater. Palaios 22, 98e103.

Bau, M., Dulski, P., 1996. Distribution of yttrium and rare-earth elements in the Penge and Kuruman iron-formations, Transvaal Supergroup, South Africa. Precambrian Research 79, 37e55.

Bodnar, R.J., 2003. Interpretation of data from aqueous-electrolyte fluid inclusions. In: Samson, I., Anderson, A., Marshal, D. (Eds.), Fluid Inclusions: Analyses and Interpretation. Short Course Series, vol. 32. Mineralogical Association of Canada, pp. 81e100.

Boyce, W.D., 1989. Early Ordovician Trilobite Faunas of the Boat Harbour and Catoche Formations (St. George Group) in the Boat Harbour-Cape Norman Area, Great Northern Peninsula, Western Newfoundland. Newfoundland Dept. of Mines and Energy, Geol. Surv. Branch, Rept. 89-2, 169 pp.

Cawood, P.A., McCausland, P.J.A., Dunning, G.R., 2001. Opening Iapetus: constraints from Laurentian margin in Newfoundland. Geological Society of America Bulletin 113, 443e453.

Clark, I.D., Fritz, P., 1997. Environmental Isotopes in Hydrogeology. Lewis Publisher, Boca Raton, FL, 328 pp.

Coleman, M.L., Walsh, J.N., Benmore, R.A., 1989. Determination of both chemical and stable isotope composition in milligram-size carbonate samples. Sedimentary Geology 65, 233e238.

Conliffe, J., Azmy, K., Knight, I., Lavoie, D., 2009. Dolomitization in the Lower Ordovician Watts Bight Formation of the St. Georges Group, western Newfoundland. Canadian Journal of Earth Sciences 46, 247e261.

Conliffe, J., Azmy, K., Gleeson, S.A., Lavoie, D., 2010. Fluids associated with hydrothermal dolomitization in St. George Group, western Newfoundland, Canada. Geofluids 9, 1–16.

Conliffe, J., Azmy, K., Greene, M., 2012. Hydrothermal Dolomites in the Lower Ordovician Catoche Formation. Marine and Petroleum Geology 30, 161–173.

Cooper, M., Weissenberger, J., Knight, I., Hostad, D., Gillespie, D., Williams, H., et al., 2001. Basin evolution in western Newfoundland: new insights from hydrocarbon exploration. American Association of Petroleum Geologists (AAPG) Bulletin 85, 393–418.

Davies, G.R., Smith, L.B., 2006. Structurally controlled hydrothermal dolomite reservoir: an overview. The American Association of Petroleum Geologists Bulletin 90, 1641–1690.

Dravis, J.J., 1992. Burial Dissolution in Limestones and Dolomites–Criteria for Recognition and Discussion of Controls: a Case Study Approach (Part 1): Upper Jurassic Haynesville Limestones, East Texas; Part 2: Devonian Upper Elk Point Dolomites, Western Canada. American Association of Petroleum Geologists–Canadian Society of Petroleum Geologists Short Course on Subsurface Dissolution Porosity in Carbonates, Calgary, Canada, 171 pp.

Esteban, M., Taberner, C., 2003. Secondary porosity development during late burial in carbonate reservoirs as a result of mixing and/or cooling of brines. Journal of Geochemical Exploration 78–79, 355–359.

Fowler, M.G., Hamblin, A.P., Hawkins, D., Stasiuk, L.D., Knight, I., 1995. Petroleum geochemistry and hydrocarbon potential of Cambrian and Ordovician rocks of western Newfoundland. Bulletin of Canadian Petroleum Geology 43, 187–213.

Giggenbach, W.F., 1986. The use of gas chemistry in delineating the origin of fluids discharges over the Taupo Volcanic Zone: a review. In: International Volcanological Congress, Hamilton, New Zealand. Proceedings Symposium, vol. 5, pp. 47–50.

Gillespie, H., Burden, E.T., 2010. Fluorescence Microspectroscopy as a Proxy to Determining the Thermal Maturation and API Gravity of Naturally Occurring Crude Oils. Internal Report CREAIT Network. Memorial University of Newfoundland, 9 pp.

Goldstein, R.H., Reynolds, T.J., 1994. Systematics of Fluid Inclusions in Diagenetic Minerals. Society for Sedimentary Geology (SEPM) Short Course, Tulsa, Okla.

Greene M., 2008. Multiple generations of dolomitization in the Catoche formation of Port au Choix Newfoundland. Unpublished M.Sc. thesis, Memorial University of Newfoundland, St. John's Newfoundland.

Hayes, P.D., Grossman, E.X., 1991. Oxygen isotopes in meteoric calcite cements as indicators of continental paleoclimate. Geology 19, 441–444.

Haywick, D.W., 1984. Dolomite Within the St. George Group (Lower Ordovician), Western Newfoundland. Unpublished M.Sc. thesis, Memorial University of Newfoundland, St. John's Newfoundland.

Iannace, A., Cupuano, M., Galluccio, L., 2011. "Dolomites and dolomites" in Mesozoic platform carbonates of the Southern Apennines: geometric distribution, petrography and geochemistry. Palaeogeography, Palaeoclimatology, Palaeoecology 310, 324–339.

James, N.P., Choquette, P.W., 1984. Diagenesis 9-Limestones e the meteoric diagenetic environment. Geoscience Canada 11, 161–194.

James, N.P., Stevens, R.K., Barnes, C.R., Knight, I., 1989. Evolution of a Lower Paleozoic continental-margin carbonate platform, northern Canadian Appalachians. In: Crevello, P.D., Wilson, J.L., Sarg, J.F., Read, J.F. (Eds.), Controls on Carbonate Platform and Basin Development. Society of Economic Paleontologists and Mineralogists Special Publication, vol. 44, pp. 123–146.

Ji, Z., Barnes, C.R., 1989. Conodont Paleontology and Biostratigraphy of the St. George Group, Lower Ordovician, Western Newfoundland, Annual Mtg. Geol. Assoc. Can., Montreal, Prog. with Abstr., p. A15.

Ji, Z., 1989. Lower Ordovician Conodonts From the St. George Group of Port au Port Peninsula, Western Newfoundland. Unpubl. Ph.D. thesis, Memorial University of Newfoundland.

Kamber, B.S., Webb, G.E., 2001. The geochemistry of late Archean microbial carbonate: implications for ocean chemistry and continental erosion history. Geochimica et Cosmochimica Acta 65, 2509–2525.

Kırmacı, M.Z., 2008. Dolomitization of the late Cretaceous–Paleocene platform carbonates, Gölköy (Ordu), eastern Pontides, NE Turkey. Sedimentary Geology 20, 289–306.

Knight, I., James, N.P., 1987. The stratigraphy of the Lower Ordovician St. George Group western Newfoundland: the interaction between eustasy and tectonics. Canadian Journal of Earth Sciences 24, 1927–1951.

Knight, I., James, N.P., Lane, T.E., 1991. The Ordovician St. George Unconformity, northern Appalachians: the relationship of plate convergence at the St. Lawrence Promontory to the Sauk/Tippecanoe sequence boundary. Geological Society of America Bulletin 103, 1200–1225.

Knight, I., Azmy, K., Greene, M., Lavoie, D., 2007. Lithostratigraphic Setting of Diagenetic, Isotopic, and Geochemistry Studies of Ibexian and Whiterockian Carbonates of the St. George and Table Head Groups in Western Newfoundland. In: Current Research Newfoundland and Labrador. Department of Natural Resources Geological Survey, Report 07-1, pp. 55–84.

Knight, I., Azmy, K., Boyce, D., Lavoie, D., 2008. Tremadocian Carbonates of the Lower St. George Group, Port au Port Peninsula, Western Newfoundland: Lithostratigraphic Setting of Diagenetic, Isotopic, and Geochemistry Studies. In: Current Research. Newfoundland and Labrador. Department of Natural Resources Geological Survey, Report 08-1, pp. 1–43.

Knight, I., 1986. Ordovician Sedimentary Strata of the Pistolet Bay and Hare Bay Area, Great Northern Peninsula. In: Current Research. Newfoundland Department of Energy and Mines, Report 86-1, pp. 147–160.

Knight, I., 1987. Geology of Roddickton (12i/16) Map Area. In: Current Research. Newfoundland Department of Energy and Mines, Mineral Development Division, Report 87-1, pp. 343–357.

Knight, I., 1991. Geology of Cambro-Ordovician Rocks in the Port Saunders (NTS 12I/11), Castors River (NTS 12I/15), St. John Island (NTS 12I/14), and Torrent River (NTS 121/10) Map Areas. Newfoundland Department of Mines and Energy, Mineral Development Division, Report 91-4, 138 pp.

Knight, I., 1994. The Geology of Cambrian–Ordovician Platform Rocks of the Psadena Map Area (NTS 12H/4). In: Current Research. Newfoundland Department of Energy and Mines, Report 97-1, pp. 211–235.

Knight, I., 1997. Ordovician Dolomite Reservoirs of the Port aux Choix area, Western Newfoundland: Report to Hunt Oil and Pan-Canadian Petroleum. 88 pp.

Land, L.S., 1967. Diagenesis of skeletal carbonates. Journal of Sedimentary Petrology 37, 914–930.

Land, L.S., 1983. The application of stable isotopes to studies of the origin of dolomite and to problems of diagenesis of clastic sediments. In: Arthur, M.A., Anderson, T.F., Kaplan, I.R., Veizer, J., Land, L.S. (Eds.), Society for Sedimentary Geology (SEPM) Short Course Notes 10, pp. 4.1–4.22.

Land, L.S., 1992. The dolomite problem: stable and radiogenic isotope clues. In: Clauer, N., Chaudhuri, S. (Eds.), Isotopic Signature of Sedimentary Records. Lecture Notes in Earth Science, vol. 43, pp. 49–68.

Lane, T.E., 1990. Dolomitization, Brecciation and Zinc Mineralization and Their Paragenetic Stratigraphic and Structural Relationships in the Upper St. George Group (Ordovician) at Daniel's Harbour, Western Newfoundland. Unpublished Ph.D. thesis, Memorial University of Newfoundland, St. John's, Nfld.

Lavoie, D., Chi, G., Brennan-Alpert, P., Betrand, R., 2005. Hydrothermal dolomitization in the Lower Ordovician Romaine Formation of the Anticosti Basin: significance for hydrocarbon exploration. Bulletin of Canadian Petroleum Geology 53, 454–471.

Lavoie, D., Morin, C., Urbatsch, M., Davis, W.J., 2010. Massive dolomitization of a pinnacle reef in the Lower Devonian West Point Formation (Gaspé Peninsula, Quebec): an extreme case of hydrothermal dolomitization through fault-focused circulation of magmatic fluids. American Association of Petroleum Geologists Bulletin 94, 513–531.

Lawler, J.P., Crawford, M.L., 1983. Stretching of fluid inclusions resulting from a low-temperature microthermometric technique. Economic Geology 78, 527–529.

Lindholm, R.C., Finkelman, R.B., 1972. Calcite staining: semiquantitative determination of ferrous iron. Journal of Sedimentary Petrology 42, 239–242.

Longman, M.W., 1980. Carbonate diagenetic textures from near surface diagenetic environments. American Association of Petroleum Geologists Bulletin 64, 461–487.

Lonnee, J., Machel, H.G., 2006. Pervasive dolomitization with subsequent hydrothermal alteration in the Clarke Lake gas field, Middle Devonian Slave Point Formation, British Columbia, Canada. American Association of Petroleum Geologists Bulletin 90, 1739–1761.

Lu, F.H., Meyers, W.J., 1998. Massive dolomitization of Late Miocene carbonate platform: a case of mixed evaporate brines with meteoric water, Nijar, Spain. Sedimentology 45, 263–277.

Lucia, F.J., Major, R.P., 1994. Porosity evolution through hypersaline reflux dolomitization. In: Puser, B.H., Tucker, M.E., Zenger, D.H. (Eds.), Dolomites, a Volume in Honour of Dolomieu. International Association of Sedimentologists, Special Publication No. 21, pp. 325–341.

Matthews, R.K., 1974. A process approach to diagenesis of reefs and reef associated limestones. In: Laporte, L.F. (Ed.), Reefs in Time and Space. SEPM Spec. Pub., vol. 18, pp. 234–256.

McLennan, S.M., 1989. Rare earth elements in sedimentary rocks: influence of provenance and sedimentary processes. In: Lipin, B.R., McKay, G.A. (Eds.), Geochemistry and Mineralogy of Rare Earth Elements. Mineral. Soc. Am. Rev. Miner., vol. 21, pp. 169–200.

Meyers, W.J., Lu, F.H., Zachariah, J.K., 1997. Dolomitization by mixed evaporative brines and freshwater, Upper Miocene carbonates, Nijar, Spain. Journal of Sedimentary Research 67, 898–912.

Möller, P., 2000. Rare earth elements and yttrium as geochemical indicators of the source of mineral and thermal waters. In: Stober, I., Bucher, K. (Eds.), Hydrology of Crystalline Rocks. Kluwer Acad. Press, pp. 227–246.

Moore, C.H., 1997. Carbonate Diagenesis and Porosity. In: Developments in Sedimentology, vol. 46. Elsevier science B.V., Amsterdam, Netherlands.

Norman, D.I., Blamey, N.J.F., 2001. Quantitative analysis of fluid inclusion volatiles by a two mass spectrometer system. In: Noronha, F., Doria, A., Guedes, A. (Eds.), European Current Research On Fluid Inclusions, Porto 2001 (XVI ECROFI): Faculdidade de Ciencias do Porto, Departamento de Geologia, Memoria no 7, pp. 341–344.

Norman, D.I., Moore, J.N., 1999. Methane and Excess N_2 and Ar in Geothermal Fluid Inclusions. In: Proceedings: Twenty-fourth Workshop of Geothermal Reservoir Engineering. Stanford University, Stanford, California, pp. 233–240.

Norman, D.I., Moore, J.N., 2003. Organic Species in Geothermal Waters in Light of Fluid Inclusion Gas Analyses. In: Proceedings, Twenty-eighth Workshop on Geothermal Reservoir Engineering. Stanford University, Stanford, California. SGP-TR-173.

Norman, D.I., Moore, J.N., Yonaka, B., Musgrave, J., 1996. Gaseous Species in Fluid Inclusions: a Tracer of Fluids and in Indicator of Fluid Processes. In: Proceedings: Twenty-first Workshop of Geothermal Reservoir Engineering. Stanford University, Stanford, California, pp. 233–240.

Norman, D.I., Moore, J.N., Musgrave, J., 1997. More on the Use of Fluid Inclusion Gaseous Species as Tracers in Geothermal Systems. In: Proceedings: Twenty-

second Workshop on Geothermal Reservoir Engineering. Stanford University, Stanford, California, pp. 419e426.
Norman, D.I., Blamey, N.J.F., Moore, J.N., 2002. Interpreting Geothermal Processes and Fluid Sources from Fluid Inclusion Organic Compounds and CO_2/N_2 Ratios. In: Proceedings, Twenty-seventh Workshop on Geothermal Reservoir Engineering. Stanford University, Stanford, California, pp. 419e426.
Nothdurft, L.D., Webb, G.E., Kamber, B.S., 2004. Rare earth element geochemistry of Late Devonian reefal carbonates, Canning Basin, Western Australia: confirmation of a seawater REE proxy in ancient limestones. Geochimica et Cosmochimica Acta 68, 263e283.
Nowlan, G.S., Barnes, C.R., 1987. Thermal maturation of Paleozoic strata in Eastern Canada from conodont colour alteration index (CAI) data with implications for burial history, tectonic evolution, hotspot tracks and mineral and hydrocarbon exploration. Bulletin e Geological Survey of Canada 367, 47.
Parry, W.T., Blamey, N.J.F., 2010. Fault fluid composition from fluid inclusion measurements, Laramide age Uinta thrust fault, Utah. Chemical Geology 278, 105e119.
Radke, B.M., Mathis, R.L., 1980. On the formation and occurrence of saddle dolomite. Journal of Sedimentary Petrology 50, 1149e1168.
Rameil, N., 2008. Early diagenetic dolomitization and dedolomitization of Late Jurassic and earliest Cretaceous platform carbonates: a case study from the Jura Mountains (NW Switzerland, E France). Sedimentary Geology 212, 70e85.
Roedder, E., 1984. Fluid Inclusions. In: Reviews in Mineralogy, vol. 12. Mineralogical Society of America, 644 pp.
Romanek, C.S., Grossman, E.L., Morse, J.W., 1992. Carbon isotopic fractionation in synthetic aragonite and calcite e effects of temperature and precipitation rate. Geochimica et Cosmochimica Acta 56, 419e430.
Scherer, M., Seitz, H., 1980. Rare earth element distribution in Holocene and Pleistocene corals and their redistribution during diagenesis. Chemical Geology 28, 279e289.
Shaw, H.F., Wasserburg, G.J., 1985. SmeNd in marine carbonates and phosphates: implications for Nd isotopes in seawater and crustal ages. Geochimica et Cosmochimica Acta 49, 503e518.
Shepherd, T.J., Rankin, A.H., Alderton, D.H.M., 1985. A Practical Guide to Fluid Inclusions. Blackie, London.
Shields, G.A., Carden, G.A.F., Veizer, J., Meidla, T., Rong, J., Li, R.-Y., 2003. Sr, C, and O isotope geochemistry of Ordovician brachiopods: a major isotopic event around the MiddleeLate Ordovician transition. Geochimica et Cosmochimica Acta 67, 2005e2025.
Sholkovitz, E., Shen, G.T., 1995. The incorporation of rare-earth elements in modern coral. Geochimica et Cosmochimica Acta 59, 2749e2756.
Sholkovitz, E., Landing, W.M., Lewis, B.L., 1994. Ocean particle chemistry: the fractionation of rare earth elements between suspended particles and seawater. Geochimica et Cosmochimica Acta 58, 1576e1580.
Smith, L.B., 2006. Origin and reservoir characteristics of Upper Ordovician Trenton-Black River hydrothermal dolomite reservoirs in New York. Bulletin of the American Association of Petroleum Geologists 90, 1691e1718.
Sperber, C.M., Wilkinson, B.H., Peacor, D.R., 1984. Rock composition, dolomite stoichiometry, and rock/water reactions in dolomitic carbonate rocks. Journal of Geology 92 (6), 609e622.
Stockmal, G.S., Slingsby, A., Waldron, J.W.F., 1998. Deformation styles at the Appalachian structural front, western Newfoundland: implications of new industry seismic reflection data. Canadian Journal of Earth Sciences 35, 1288e1306.
Swart, P.K., Eberli, G., 2005. The nature of the delta C-13 of periplatform sediments: Implications for stratigraphy and the global carbon cycle. Sedimentary Geology 175, 115e129.
Tucker, M.E., Wright, V.P., 1990. Carbonate Sedimentology. Blackwell Publishing, Oxford, UK.
Veizer, J., Ala, D., Azmy, K., Bruckschen, P., Bruhn, F., Buhl, D., et al., 1999. $^{87}Sr/^{86}Sr$, ^{18}O and ^{13}C evolution of Phanerozoic seawater. Chemical Geology 161, 59e88.
Warren, J., 2000. Dolomite: occurrence, evolution and economically important associations. Earth-Science Reviews 52, 1e81.
Webb, G.E., Kamber, B.S., 2000. Rare earth elements in Holocene reefal microbialites: a new shallow seawater proxy. Geochimica et Cosmochimica Acta 64, 1557e1565.
Webb, G.E., Nothdurft, L.D., Kamber, B.S., Kloprogge, J.T., Zhao, J.-X., 2009. Rare earth element geochemistry of scleractinian coral skeleton during meteoric diagenesis: a before and-after sequence through neomorphism of aragonite to calcite. Sedimentology 56, 1433e1463.
Weissert, H., Michael, J., Michael, S., 2008. Chemostratigraphy. Newsletter on Stratigraphy 42, 145e179.
Weyl, P.K., 1960. Porosity through dolomitization: conservation of mass requirements. Journal of Sedimentary Petrology 30, 85e90.
Wierzbicki, R., Dravis, J.J., Al-Aasm, I., Harland, N., 2006. Burial dolomitization and dissolution of Upper Jurassic Abenaki platform carbonates, Deep Panuke reservoir, Nova Scotia, Canada. American Association of Petroleum Geologists Bulletin 90, 1843e1861.
Wilde, P., Quinby-Hunt, S.M., Erdtmann, B.D., 1996. The whole-rock cerium anomaly: a potential indicator of eustatic sea-level changes in shales of the anoxic facies. Sedimentary Geology 101, 43e53.
Williams, S.H., Burden, E.T., Mukhopadhyay, P.K., 1998. Thermal maturity and Burial history of Paleozoic rocks in western Newfoundland. Canadian Journal of Earth Sciences 35, 1307e1322.
Wilson, J.L., Medlock, P.L., Fritz, R.D., Canter, K.L., Geesaman, R.G., 1992. A review of Cambro-Ordovician breccias in North America. In: Candelaria, M.P., Reed, C.L. (Eds.), Paleokarst, karst-related diagenesis and reservoir development. SEPM-Permian Basin Section, Publication 92-33, pp. 19e29.
Zhang, S., Barnes, C.R., 2004. Arenigian (Early Ordovician) sea-level history and the response of conodont communities, western Newfoundland. Canadian Journal of Earth Sciences 41, 843e865.
Zhong, S., Mucci, A., 1995. Partitioning of rare earth elements (REEs) between Calcite and seawater solutions at 25 °C and 1 atm, and high dissolved REE concentrations. Geochimica et Cosmochimica Acta 59, 443e453.